

Material Science and Technology Division

**Propulsion Materials Program
Quarterly Progress Report for
April through June 2008**

**D. R. Johnson
Technical Project Manager**

**Prepared for
U.S. Department of Energy
Assistant Secretary for Energy Efficiency and Renewable Energy
Office of Vehicle Technologies Program
VT 05 04 000**

**Prepared by the
OAK RIDGE NATIONAL LABORATORY
Oak Ridge, Tennessee 37831-6066
Managed by
UT-Battelle, LLC
for the Department of Energy
Under contract DE-AC05-00OR22725**

CONTENTS

Project 18516 – Materials for Electric and Hybrid Drive Systems

Agreement 16307 – Modeling/Testing of Environmental Effects on PE Devices (ORNL)

Agreement 16305 – Materials by Design – Solder Joint Analysis (ORNL)

Agreement 16306 – Materials Compatibility of Power Electronics (ORNL)

Project 18517 – Combustion System Materials

Agreement 11752 – Advanced Materials Development through Computational Design for HCCI Engine Applications (ORNL)

Agreement 8697 – Electrochemical NO_x Sensor for Monitoring Diesel Emissions (LLNL)

Agreement 9440 – Fabrication of Micro-orifices for Diesel Fuel Injectors (ANL)

Agreement 11754 – Hydrogen Materials Compatibility (PNNL)

Project 18518 – Materials for High Efficiency Engines

Agreement 16304 – Materials for Advanced Engine Valve Train CRADA with Caterpillar (ORNL)

Agreement 13329 – Mechanical Reliability of PAT Piezo-Stack Actuators For Fuel Injectors (ORNL)

Agreement 13332 – Friction and Wear Reduction in Diesel Engine Valve Trains (ORNL)

Agreement 9089 – NDE of Diesel Engine Components (ANL)

Project 18519 – Materials for Control of Exhaust Gases and Energy Recovery Systems

Agreement 9130 - Development of Materials Analysis Tools for Studying SCR CRADA with Cummins (ORNL)

Agreement 10461 - Durability and Reliability of Ceramic Substrates for Diesel Particulate Filters (ORNL)

Agreement 10635 – Catalysis by First Principles - Can Theoretical Modeling and Experiments Play a Complimentary Role in Catalysis? (ORNL)

Project 18865 – Materials by Design

Agreement 9105 – Ultra-High Resolution Electron Microscopy for Characterization of Catalyst Microstructures and De-activation Mechanisms (ORNL)

Agreement 9110 – Life Prediction for Diesel Engine Components (ORNL)

Agreement 14957 – Thermoelectrics Modeling (ORNL)

Agreement 16308 – Thermoelectric Materials (ORNL)

Agreement 16307: Modeling/Testing of Environmental Effects on PE Devices

**A. A. Wereszczak, K. Lowe, O. M. Jadaan, T. P. Kirkland, and M. Lance
Oak Ridge National Laboratory**

Objective/Scope

Understand the complex relationship between environment (temperature, humidity, and vibration) and the performance and reliability of the material constituents within automotive power electronic (PE) devices. There is significant interest in developing more advanced PE devices and systems for transportation applications (e.g., hybrid electric vehicles, plug-in hybrids) that are capable of sustained operation to 200°C. Advances in packaging materials and technology can achieve this but only after their service limitations are better understood via modeling and testing.

Technical Highlights

Two primary efforts continued during the present report period. They were the mechanical and electrical evaluation of candidate or alternative ceramics for use in a direct copper bonded (DCB) substrate, and the collaboration with the NTRC group of R. Wiles, C. Ayers, and K. Lowe in the development of a direct-cooled PE device.

Evaluation of Alternative Ceramic Substrates

Several electronic ceramic materials are undergoing equibiaxial (ball-on-ring) flexure in air, and while submerged in 50% water - 50% ethylene glycol or 100% water environments. A 96% alumina, a 99.6% alumina, an aluminum nitride, a silicon nitride, a boron nitride, and a polycrystalline silicon carbide are under evaluation. Tests in the two non-air environments are being performed to get a sense of any strength degradation or longer-term chemical incompatibility for consideration of the direct-cooled PE device portion of this project.

An exposure test rig was fabricated that will enable the candidate substrate materials to be subjected to long-term coolant fluid impingement. Fluids are to be 50/50 WEG and 100% water. After their exposure, specimens will be examined for evidence of erosion and strength degradation.

A developmental, high-resistivity ($> 10^8 \Omega \cdot \text{cm}$) polycrystalline silicon carbide is still under consideration for electrical insulation candidacy in this project. Many of its properties make it attractive for use in DBCs. High electrical resistivities have been confirmed and breakdown voltage tests are to be commenced. Specimens for thermal conductivity tests are now being machined and will be used to measure (and hopefully confirm) the anticipated high thermal conductivity.

Direct-Cooled PE Device

Stress analysis of a direct-cooled alumina ceramic substrate and its probability of survival were estimated. This analysis is illustrated in Figs. 1-8. Only one twelfth of the

entire component was modeled owing to symmetry, and its layout is shown in Fig. 1. The model is comprised of four subcomponents each made from different materials, and the properties used for each are shown in Fig. 2. ORNL/NTRC's K. Lowe supplied axial temperature profiles and they were applied as a boundary condition as shown in Fig. 3. The resulting temperature profiles for the model and the four material constituents are shown in Figs. 4-5. Using those temperature profiles and the properties listed in Fig. 2, the resulting first principal stress fields in two brittle material constituents (the alumina substrate and the silicon chip) were then analyzed (see Fig. 6). In order to combine the first principal tensile stress field with Weibull strength distribution of the alumina, the effective area and volume (as a function of Weibull modulus) needed to first be determined, and those results are shown in Fig. 7. Using those results and reasonable Weibull properties for alumina, the probability of survival of the alumina substrate was finally able to be estimated, and that outcome is shown in Fig. 8. There is very low probability of failure for the alumina substrate subjected to those service conditions.

Status of FY 2008 Milestones

Establish controlled environmental test facility that can controllably subject PE devices to concurrent temperature, humidity, and vibration conditions. [Sep08]. *On schedule.*

Communications/Visits/Travel

Pertaining to the substrate-related efforts, numerous discussions were held with Kyocera's Adam Schubring, Ceradyne's Biljana Mikijelj, and Saint-Gobain's John Bevilacqua. Regarding the PE-direct-cooling efforts, numerous discussions and visits occurred with NTRC's Randy Wiles, Curt Ayers, and Kirk Lowe.

Problems Encountered

None.

Publications/Presentations/Awards

None.

References

None.

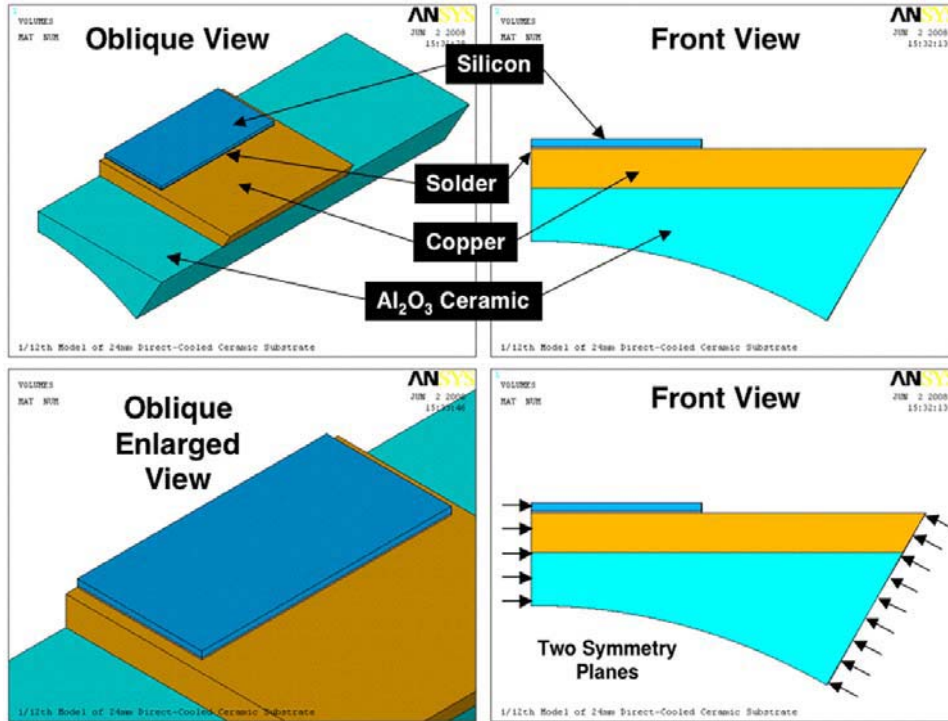


Figure 1. One-twelfth model of direct-cooled ceramic substrate.

Material	E (GPa)	Poisson's Ratio	CTE (ppm/°C)	κ (W/mK)	Yield Strength (MPa)
Al ₂ O ₃	360	0.24	8	25	
Copper	117	0.30	17	400	138
Solder	12.5	0.36	26	15	22
Silicon	130	0.28	4	130	

Figure 2. Values of properties used for the model's four material constituents.

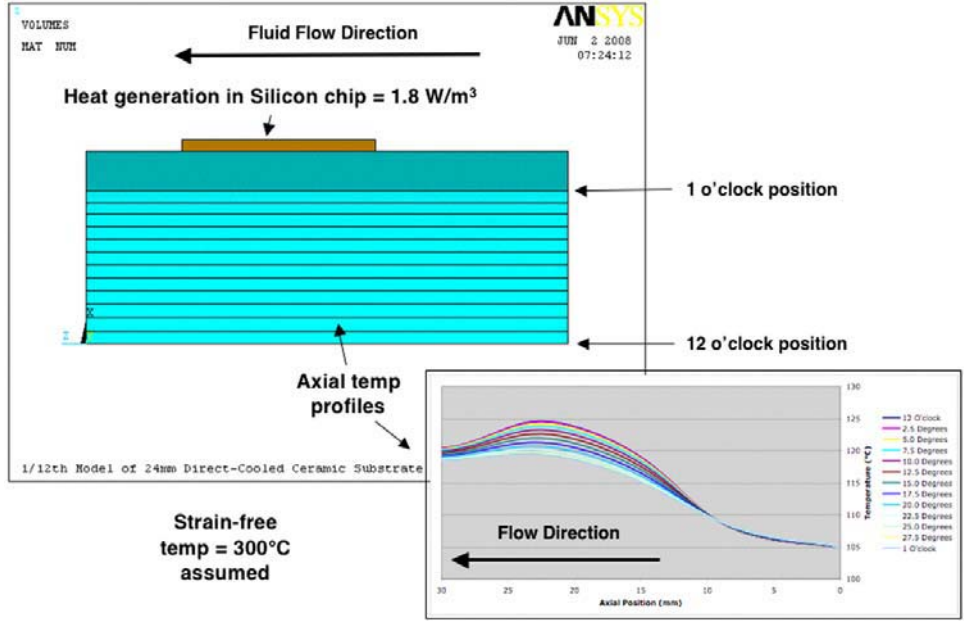


Figure 3. Thermal boundary conditions used in the analysis.

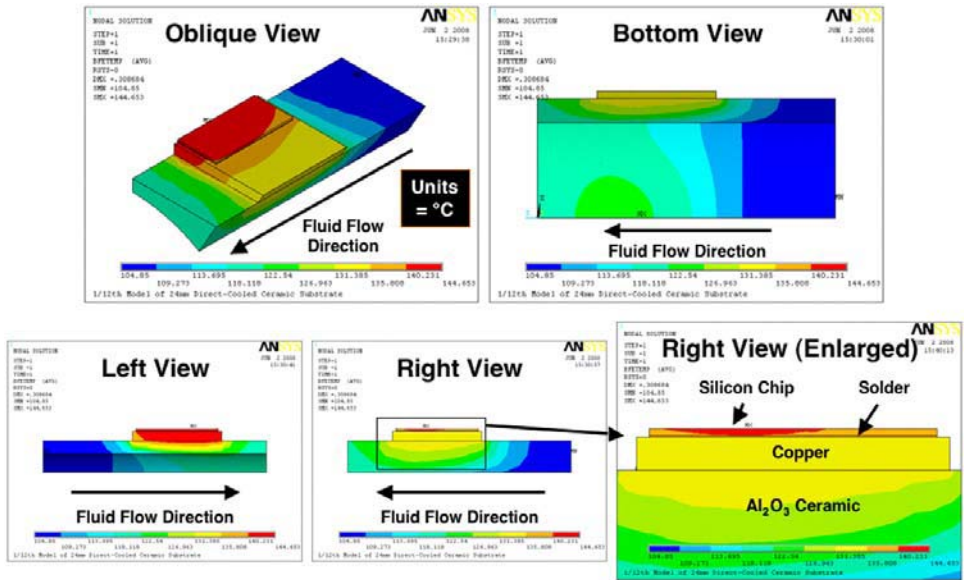


Figure 4. Produced temperature profiles in the model.

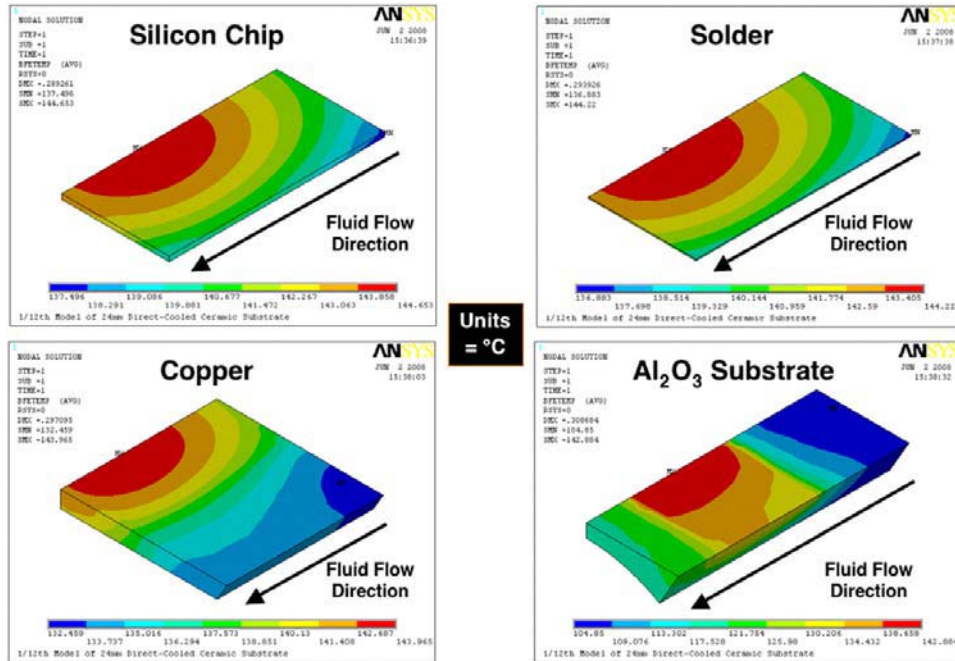


Figure 5. Produced temperature the four material constituents.

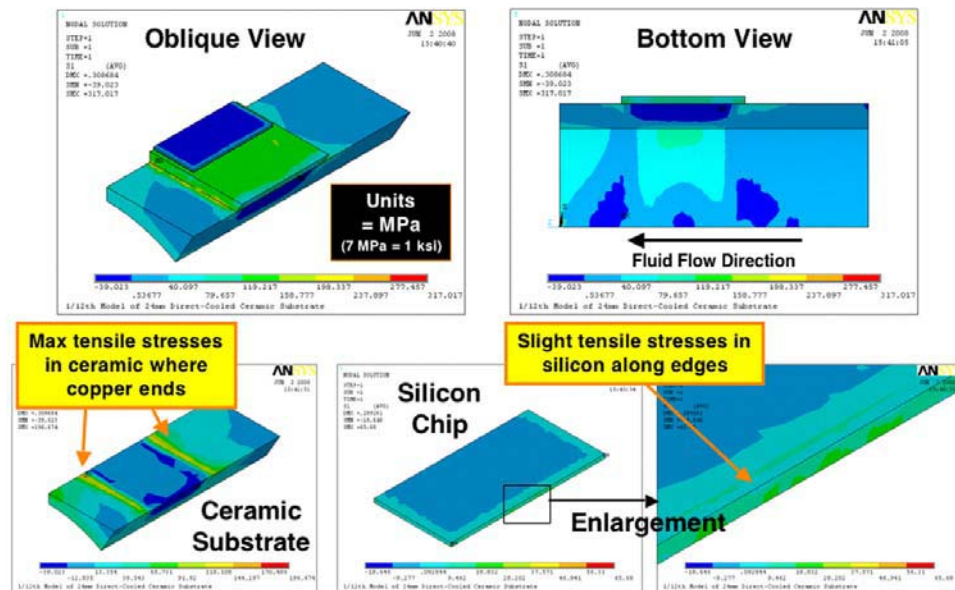


Figure 6. First principal stress fields in the ceramic substrate and silicon chip.

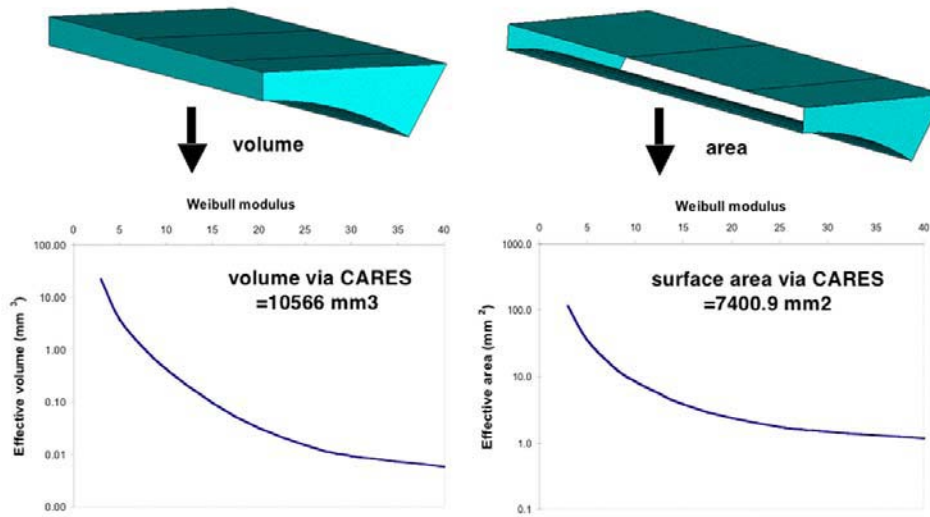


Figure 7. Estimated effective volume and effect area for the alumina substrate.

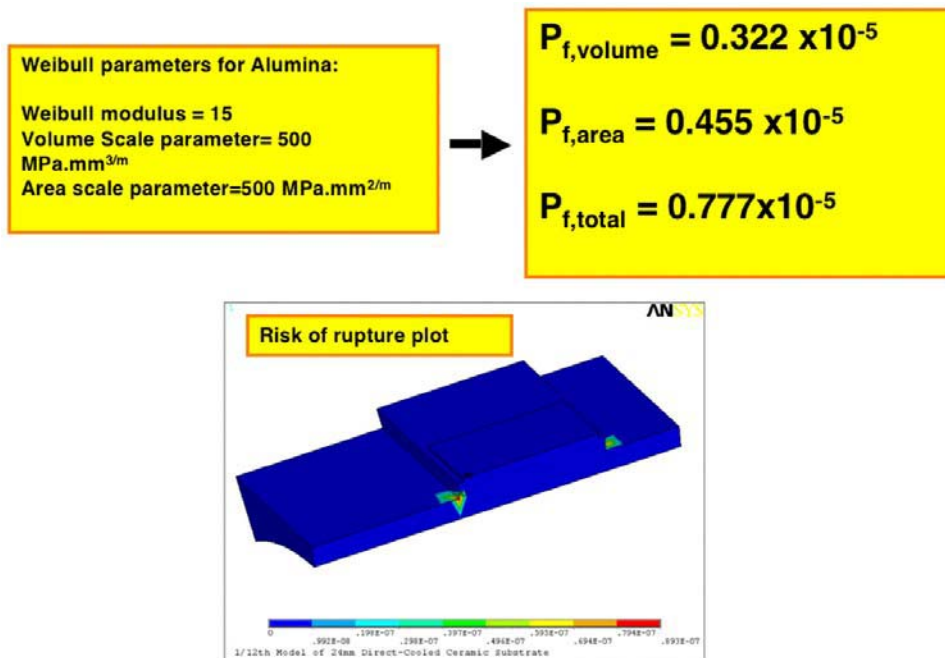


Figure 8. Resulting probability of failure in the alumina substrate.

Agreement 16305: Materials By Design: Solder Joint Analysis

**G. Muralidharan, Andrew Kercher, Larry Seiber, and Burak Ozpineci
Oak Ridge National Laboratory**

Objective/Scope

Advanced hybrid and electric propulsion systems are required to achieve the desired performance and life targets set for future automobiles. As specified in the OFCVT objectives, a target lifetime of 10-15 years has been projected for hybrid and electric propulsion systems meant for operation in harsh automotive environments. Power electronic components and systems are integral components of advanced automotive hybrid and electric propulsion systems. The trend in automotive power electronics is for using higher operating temperatures which has a detrimental effect on the stability of materials used in such systems. The objective of this task is to evaluate the effects of the higher temperatures on critical metallic materials that are used in power electronic devices and systems and to use the Materials-by-Design approach to identify appropriate combinations of materials that would decrease inopportune failures and maximum lifetime and reliability.

Based on the trend for using higher temperatures in power electronic components, there is a significant need to study failures of electronic packages induced by metallurgical changes of solder joints used as die attaches, and in wire bonds exposed to high temperatures (up to 200°C in contrast to the current 125-150°C exposure) anticipated in such applications. These failures can be induced in solder joints and other components by combination of temperatures, stresses, and current. Coarsening of solder joint microstructure along with the formation of intermetallic compounds takes place during high temperature exposure. Wire bonds are also known to be a key location of failures for packages meant for high temperature use. An understanding of the failures in solder joints and wire bonds will empower us to develop a computation-oriented method for the design of materials for packaging applications.

The approach used in this work would be to study failures in simple package designs so that the emphasis is on materials rather than package design thus avoiding complexities of package design issues that may overshadow materials issues. Packages will be subject to extremes of operational stress levels/temperature levels to the study the origin of failures. Steady-state exposure at high temperatures and cyclic exposures (thermal fatigue) all affect microstructure of the materials, their properties, and hence the failure of joints. X-ray radiography along with acoustic and infrared imaging (as is necessary) will be used to characterize voids present in the solder joints. Knowledge from the failures would enable the selection/development of more appropriate materials that would ensure required lifetimes of 10 to 15 years expected of modules in EVs and Hybrid systems.

Technical Highlights

In this quarter, progress has been made in conducting the first thermal cycling tests on a commercial package. The test chamber EC11A capable of exposing packages to temperatures up to 315°C for long times and to thermal cycling between 315°C and -184°C now available at ORNL was used for the thermal cycling tests. Figure 1 shows a

plot of the temperature vs. time curve obtained during a thermal cycling test from -65°C to 150°C conducted on one 600-V diode module (Part # QRC 0640T30) obtained from PowerEx . Three different temperatures are shown on the plot; the target temperature for that particular cycle, temperature of the chamber, and actual temperature experienced by the part. These tests have been conducted according to the JEDEC standards for thermal cycling.

Figures 2(a) and 2 (b) show an example of the forward and reverse characteristics obtained from one of the diode modules. Electrical characteristics of the diode modules were measured after 10 and 20 thermal cycles and compared to the diode tested in the as-received condition. Figure 3 shows the resistance observed in the forward characteristics of two diodes in the tested package. It is clearly seen that the thermal cycling affects the electrical properties of the joints in the package. Further work will be carried out to study failure in one of the joints in commercial or a test joint.

Status of FY 2008 Milestones

Work is on schedule to meet the following milestone.

Evaluate microstructural evolution and causes related to the failure of one most commonly used solder in a selected high temperature package when subjected to stress testing conditions. **(9/08)**

Communications/Visits/Travel

Several non-functional SiC devices have been obtained from SemiSouth for fabrication of die attach joints with a DBC substrate. Communications are being carried out with PowerEx about the feasibility of fabrication of simple packages consisting of solder joints with zero void content at their manufacturing facility.

Problems Encountered

Publications/Presentations/Awards

None

References

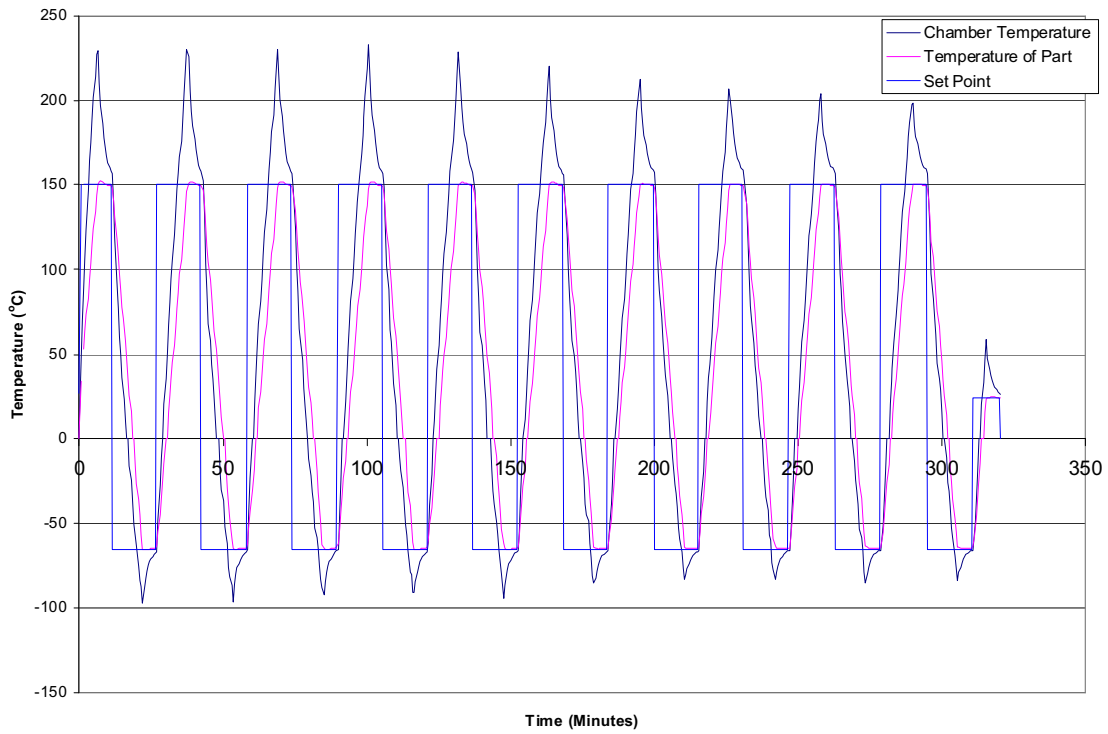


Figure 1. Time dependent profile of temperatures in thermal cycling tests conducted on one package. The red curve shows the temperatures experienced by the device under test.

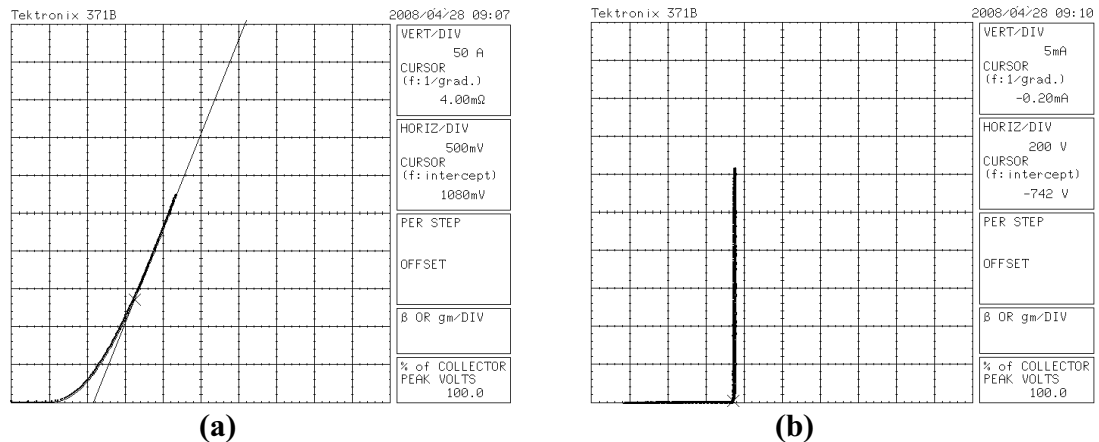


Figure 2. Typical electrical properties obtained from the tested diodes; (a) forward characteristics, and (b) reverse characteristics. Effect of temperature cycling on these characteristics were evaluated, with particular reference to the resistance measured in the forward characteristics (inverse of the slope of the linear portion of the curve shown in figure a) and the blocking voltage in the reverse characteristics.

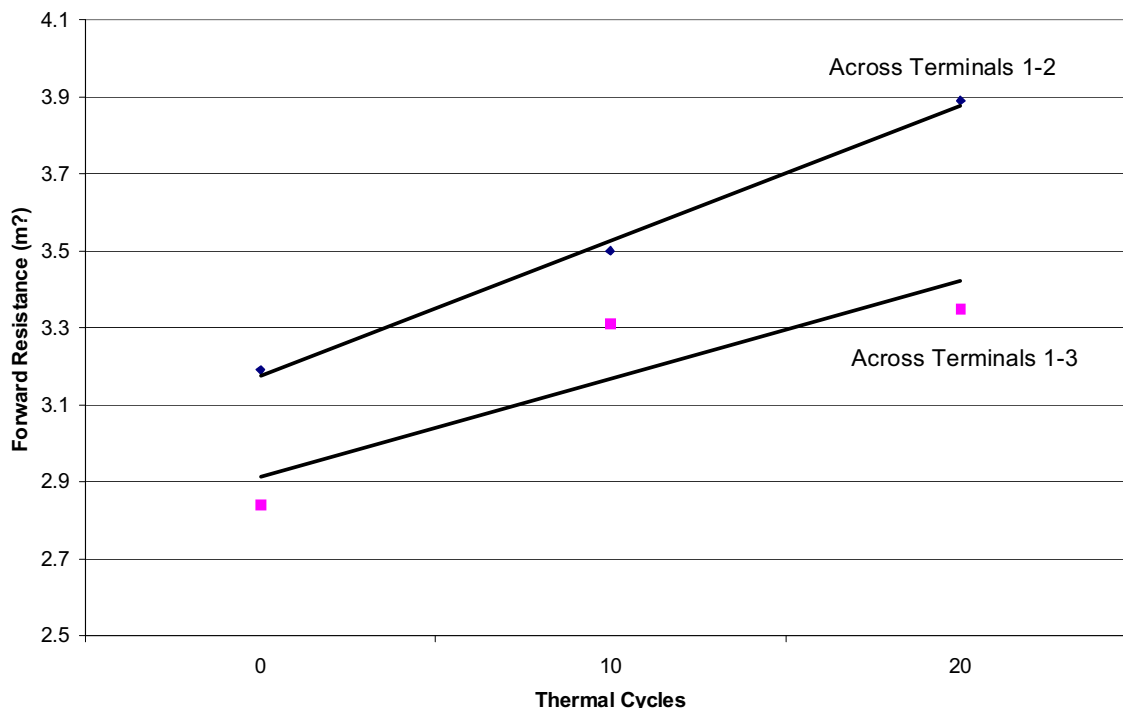


Figure 3. Thermal cycling resulted in a gradual increase in the forward resistance in two different diodes located in the same package.

Agreement 16306: Materials Compatibility of Power Electronics

**B. L. Armstrong, D. F. Wilson, C. W. Ayers, and S. J. Pawel
Oak Ridge National Laboratory**

Objective/Scope

The use of evaporative cooling for power electronics has grown significantly in recent years as power levels and related performance criteria have increased. As service temperature and pressure requirements are expanded, there is concern among the Original Equipment Manufacturers (OEMs) that the reliability of electrical devices will decrease due to degradation of the electronic materials that come in contact with the liquid refrigerants. Potential forms of degradation are expected to include corrosion of thin metallic conductors as well as physical/chemical deterioration of thin polymer materials and/or the interface properties at the junction between dissimilar materials in the assembled components. Initially, this new project will develop the laboratory methodology to evaluate the degradation of power electronics materials by evaporative liquids.

Technical Highlights

Candidate power electronic components were obtained. These simplified circuits will be used to perform an initial evaluation of the proposed methodology for examining the interaction of the electrical components with evaporative direct cooling fluids. Pre-exposure surface characterization of the circuits was performed. The typical appearance of the circuits is shown in Fig. 1. As shown, each circuit is composed of six wires, which are bonded to the board. The bonds all show uniform contact area and deformation associated with the bonding process. Test cells and associated cooling/recirculating systems are being prepared.

Status of FY 2008 Milestones

Develop the methodology to examine the interaction of the electrical components with the fluids used in the evaporative cooling systems. **(09/08)** On track.

Communications/Visits/Travel

None to report.

Problems Encountered

None to report.

Publications/Presentations/Awards

None to report.

References

None to report.

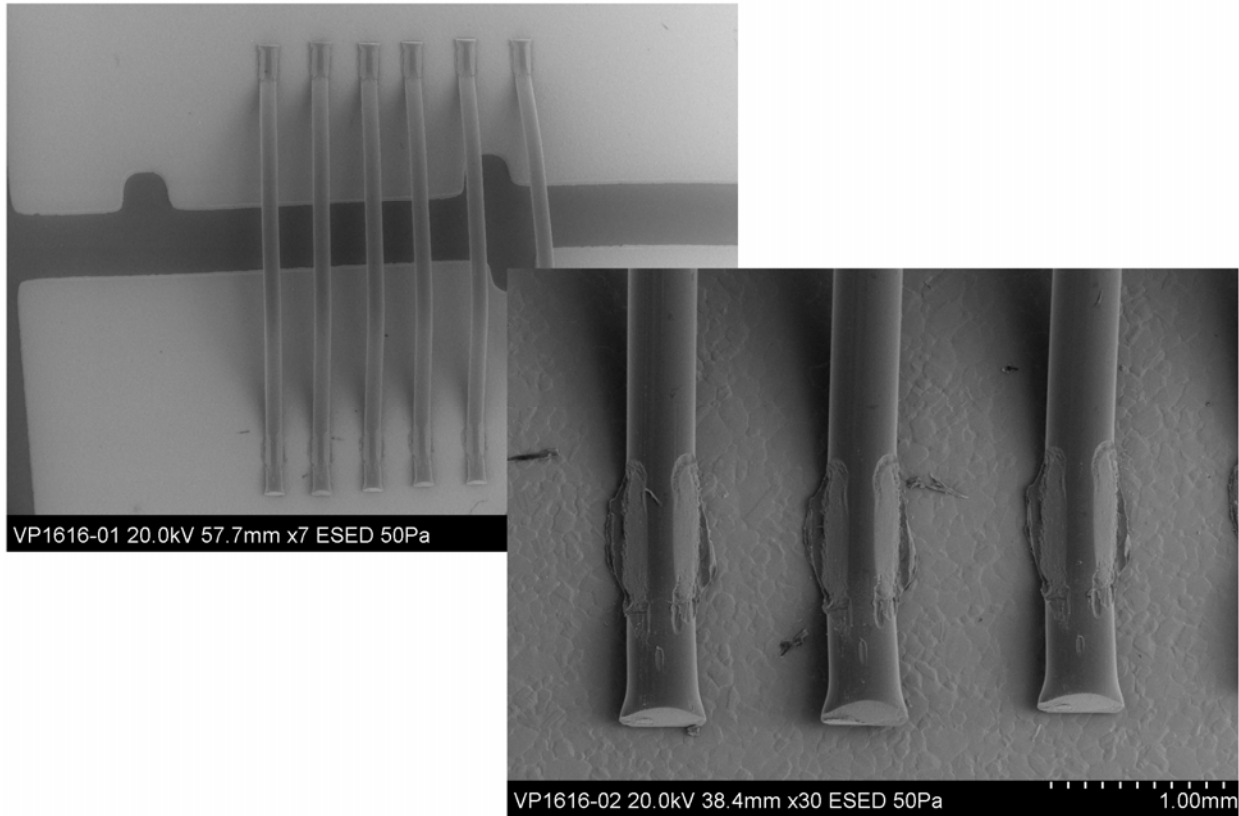


Figure 1. Typical appearance of six-wire test circuit. The bond regions show uniform contact area and deformation associated with the bonding process.

Agreement 11752: Advanced Materials Development through Computational Design for HCCI Engine Applications

**Vinod K. Sikka, Govindarajan Muralidharan, Rick Battiste, and Bruce G. Bunting
Oak Ridge National Laboratory**

Objectives/Scope

To identify and catalog the materials operating conditions in the HCCI engines and utilize computational design concepts to develop advanced materials for such applications.

Highlights

Technical Progress

Materials-by-Design of Advanced Materials:

In this quarter, work was continued on Ni-based alloys for valve applications. As reported earlier, using thermodynamic modeling, microstructure evaluation, and mechanical property evaluation, high temperature fatigue was identified as a property of critical interest in Ni-based alloy valve materials for the next generation automotive engines. An important part of the on-going work is to develop a database of mechanical properties as a function of alloy composition and microstructure (which is a function of processing and heat-treatment). In this quarter, work was carried out on developing fatigue data on one of the alloys with the higher γ' volume fractions, Udimet 41. Figure 1 shows the fatigue life of Udimet 41 in the aged condition obtained at two different stress levels. Note that the Udimet 41 has significantly better fatigue life than IN751 under similar stress and temperature levels.

Additional emphasis was placed this quarter on microstructural characterization using SEM and TEM. Figure 2 shows representative SEM images from Udimet 720 which behaved anomalously in terms of its fatigue properties. Preliminary investigations show the likelihood of the presence of large γ' precipitates which may be the cause for reduced fatigue resistance. Further characterization work will be carried out to better guide the identification of potentially improved alloys.

Milestones

Develop material with the potential to have appropriate performance for valve application through computational modeling and experimental validation. **(9/08) (On-track)**

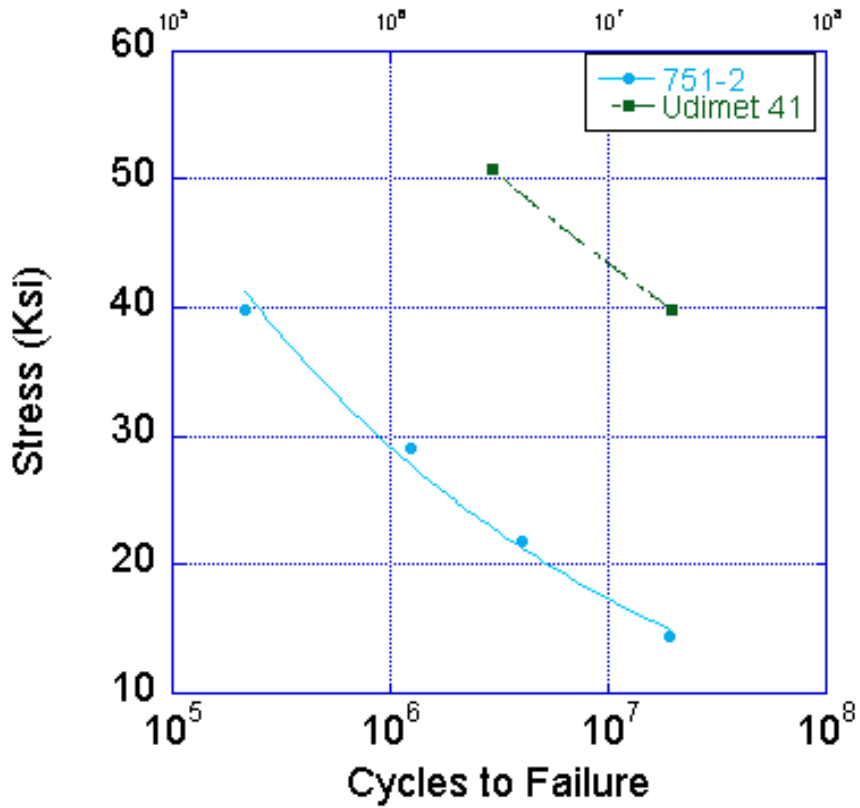
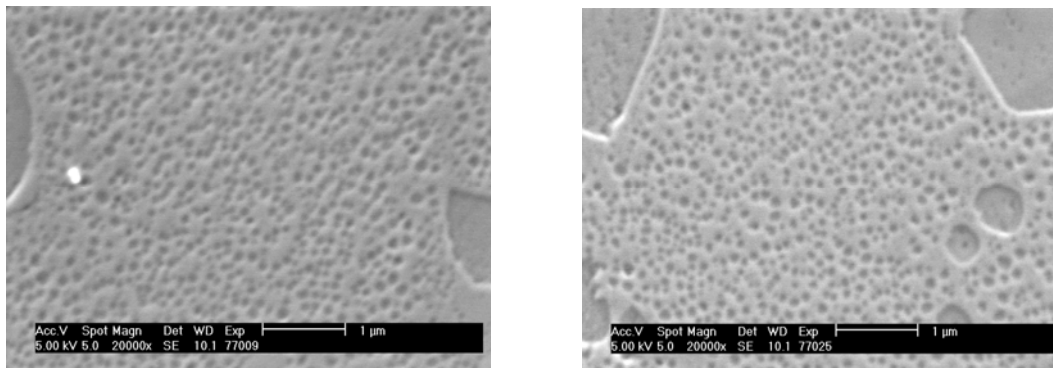


Figure 1. Fatigue life of Udimet 41 at two different stress levels at 870°C. Also shown for comparison are the fatigue lives of IN 751 under the same conditions. Lines are drawn to guide the eye.



(a)

(b)

Figure 2. SEM images showing γ' precipitates in Udimet 720 after (a) ~400 minutes and (b) ~ 6000 minutes

Agreement 8697: Electrochemical NO_x Sensor for Monitoring Diesel Emissions

**Leta Y. Woo, and Robert S. Glass
Lawrence Livermore National Laboratory**

Objective/Scope

The main goal is the development of technology for measuring NO_x in diesel exhaust using low-cost, high-sensitivity on-board sensors. Solid-state electrochemical sensors are robust and an ideal platform for exploring NO_x sensing strategies that build upon designs previously demonstrated for the detection of hydrocarbon emissions in automobile exhaust. Characterization of materials and design will be used to optimize the sensor for operation in environments comparable to the exhaust stream of the CIDI engine.

Technical Highlights

Previously, an impedance-based NO_x sensing technique was presented with laboratory prototypes demonstrating reasonable stability (~500 hours) at the operating temperature (650°C), sensor speeds less than 10 sec., sensitivity down to 5 ppm NO_x, and minimal cross-sensitivity to water at the operating temperature of 650°C. Remaining issues include cross-sensitivity to oxygen, temperature sensitivity, and long-term stability (>500 hours) as well as continuing to improve the sensor platform to be more suitable for commercialization. Current progress includes a significant improvement in the sensor platform by demonstrating a working prototype that uses an integrated (buried) heater to control the temperature at the sensor surface. The substrate with the integrated heater was provided by our collaborators at Ford. Furthermore, our collaborators at Ford were able to work with one of their U.S. suppliers to package the improved prototype sensor (which now incorporates an integrated heater) into an oxygen sensor housing. The oxygen sensor housing further demonstrates the potential commercialization of the prototype and also allows the prototype sensor to undergo more rigorous types of emission testing. Initial measurements of the prototype packaged in the oxygen sensor housing show reasonable sensitivity to NO_x. Current progress also includes continuing to characterize the most recent prototype tested at Ford, where the results will aid sensor design and improve the testing protocol of engine dynamometer experiments at Ford testing facilities. Stability testing of electronically conducting perovskite oxides continued and will be evaluated. Future work will include characterizing the prototype packaged in the oxygen sensor housing. Engine dynamometer experiments at Ford testing facilities have been tentatively scheduled for the end of the 4th quarter.

Status of FY 2008 Milestones

The 1st quarter 2008 milestones have been achieved, including dynamometer testing and progress towards further developing criteria for appropriate materials and configurations. The 2nd quarter milestones have been achieved including evaluation of conducting perovskite oxides, laboratory investigation of cross-sensitivity to interfering gases, and a presentation at the 32nd International Conference and Exposition on Advanced Ceramics and Composites. Evaluation of conducting perovskite oxides and

cross-sensitivity has continued into the 3rd quarter. The 3rd quarter milestones that have been achieved include incorporating potentially commercializable sensor fabrication techniques, which was demonstrated by building our prototype using the integrated (buried) heater provided by Ford, and then having the sensor packaged into an oxygen sensor housing by a U.S. supplier. The 3rd quarter milestone of compiling sensor performance data for varying operating parameters is ongoing and will continue into the 4th quarter.

Communications/Visits/Travel

- Bi-weekly teleconferences with Ford collaborators have continued in order to coordinate efforts in developing a deployable and commercializable NO_x sensor technology.

Publications/Presentations/Awards

- A thirty-minute oral presentation entitled "NO_x Sensor Development for Monitoring Diesel Emissions" was given by Leta Woo at LLNL during a one-day visit by USCAR (United States Council for Automotive Research) on April 23, 2008. Attendees included representatives from Chrysler, Ford, General Motors, and the DOE.

Agreement 9440: Fabrication of Micro-orifices for Diesel Fuel Injectors

**George Fenske
Argonne National Laboratory**

Objective/Scope

- Reduce soot by improving fuel dispersion using smaller injector orifices
- Develop and evaluate methods for depositing adherent coatings on the inside diameter of fuel injector orifices in order to narrow them down.
 - Size goal: Final orifice diameter of 50 μm
 - Durability goal: Coating must remain adherent after repeated thermal cycling, must be resistant to sustained temperatures $>300^{\circ}\text{C}$, and must be able to resist repeated impact loads in the needle seat area.
 - Reproducibility goal: Post-treatment orifice diameter variation must be no greater than that of the pre-treatment orifice diameter
- Evaluate the effect of coating on spray pattern.
- Test the effect of coating on deposit formation.
- Transfer developed technology to DOE industrial partners.

Technical Highlights

- Continued metallurgical evaluation of NVD coatings applied to commercial nozzles. Completed SEM analysis of chemical composition of injector nozzles

Status of FY 2008 Milestones

- Milestones on-schedule

Communications/Visits/Travel

- Teleconference with US EPA for future flow visualization studies.

Problems Encountered

- N/A

Publications/Presentations/Awards

- George Fenske, John Woodford, Jin Wang, Ronald Schaefer and Fakhri Hamady, "Fabrication and Characterization of Micro-Orifices for Diesel Fuel Injectors", 2008 SAE International Powertrains, Fuels and Lubricants Congress, Shanghai, China; Jun 23-25, 2008

Agreement 11754: Hydrogen Materials Compatibility

Chuck Henager, Jr., Stan Pitman, Joe Ryan, James Holbery
Pacific Northwest National Laboratory

Objectives

- Measure the friction and wear characteristics of injector materials in hydrogen environments, including *in-situ* and *ex-situ* materials characterization.
- Develop accelerated test methods and durability procedures for materials/coatings used on hydrogen injectors.
- Measure the performance of piezoelectric actuators and actuator materials in hydrogen environments.
- Assist in the design of the direct fuel injector for Westport-Ford through materials modeling, analysis, and selection.

Technical Highlights

- **Needle-Nozzle Friction-Wear:** We have not received Penn State sliding tests on samples designed to verify *in-situ* apparatus. We have conducted sample tests on all DLCs and nanolaminates, hydrogen pressurized DLCs and nanolaminates, and are currently exposing samples to 1000 hours hydrogen to test in the near future. *Contact: J. Holbery, 509-375-3686, james.holbery@pnl.gov.*
- **Coating Development:** DLC samples were received from Morgan Ceramics, Ion Bond, and Argonne National Lab. Samples have been tested in micro and nanoindentation, reciprocating tribology testing, have been pressurized in hydrogen, and are now being tested in sliding and Raman. Also, we have attempted to conduct quantitative sliding-impact on ANL and PNNL samples at ORNL, though we ran into equipment difficulties at PNNL. *Contact: J. Holbery, 509-375-3686, james.holbery@pnl.gov.*
- **Piezo Material Development.** Samples have not been received from either Westport or suppliers. This effort has been abandoned for FY08 due to lack of materials. *Contact: J. Holbery, 509-375-3686, james.holbery@pnl.gov.*

Status of FY 2008 Milestones

1. Complete 100% hydrogen *in-situ* sliding wear tests to quantify injector friction coefficient and resulting material embrittlement with the goal of understanding and predicting the fundamental material degradation / aging mechanisms in hydrogen service environment.

Status: Wear tests are 100% complete on base materials; coatings are 90% complete.

2. Complete 100% hydrogen *in-situ* piezo actuation tests of commercial PZT formulations, extending on the initial test plan completed in FY07.

Status: Westport and Physic Instrument did not supply PZT materials.

3. Model the diffusion of hydrogen into engine component materials via atomistic models complemented with experimental neutron backscattering data generated on component materials.

Status: Scientist (S&E 3) began in July to conduct this work; funding is nearly exhausted this year and we achieved only 25% of the milestone.

4. Complete *in-situ* and *ex-situ* sliding-impact testing of needle-seat combination to understand the failure mechanism on injector seat materials.

Status: PNNL personnel travelled to ORNL to conduct this work. The apparatus had not been used previously by either ORNL or PNNL personnel and therefore the data was not quantitative as had been planned. We made every attempt to complete this milestone but the ORNL equipment was not adequately operational to complete the full milestone..

Communications/Visits/Travel

- Trip made to ORNL to conduct nanoindentation and sliding-impact testing on coated materials. We generated approximately 1000 nanoindents on the materials, and conducted qualitative sliding-impact testing on two coatings.

Publications/Presentations/Awards

- Abstract accepted to SAE Fall 2008 titled "Challenges in Developing Hydrogen Direct Injection Technology for Internal Combustion Engines," Alan Welch, David Mumford, Sandeep Munshi, James Holbery, Brad Boyer
- Abstracts (two) accepted to 2008 Int. Hydrogen Conference, Jackson Hole, WY, Sept 2009, one for oral presentation and one poster. Both will be published in proceedings.

Agreement 16304: Materials for Advanced Engine Valve Train

**P. J. Maziasz and N. D. Evans
Oak Ridge National Laboratory**

**N. Phillips
Caterpillar, Inc.**

Objective/Scope

This is a new ORNL CRADA project with Caterpillar, NFE-07-00995 and DOE OVT Agreement 16304, that began earlier this year, and lasts for about 2.5 years. This CRADA project is focused on addressing the wear and failure modes of current on-highway heavy-duty diesel exhaust valves and seats, and then evaluating changes in valve-seat design and advanced alloys which enable higher temperature capability, as well as better performance and durability. Requests for more detailed information on this project should be directed to Caterpillar, Inc.

Highlights

Caterpillar, Inc.

Caterpillar completed testing and characterization on an initial set of exhaust valves and their matching seats previously, and then provided fresh exhaust valves and seats to match with those wear-tested in the lab-test rig to ORNL for further analyses. This quarter, Caterpillar conducted wear resistance tests, fractographic examinations of plate and pin wear specimens, and a seat insert temperature analysis.

ORNL

ORNL conducted in depth microcharacterization studies of non-wear valve seat components. Combined SEM and XPS studies of surface oxides and sub-surface regions were completed to benchmark microstructures developed during specific aging schedules.

Technical Progress, 3rd Quarter, FY2008

Background

This is a new ORNL CRADA project with Caterpillar, NFE-07-00995 and DOE, OVT Agreement 16304, which began earlier this year, and will last for about 2.5 years. This CRADA project is focused on addressing the wear and failure modes of current on-highway heavy-duty diesel exhaust valves and seats, and then on evaluating changes in valve-seat design and/or advanced alloys that enable higher temperature capability, as well as better performance and durability. The need for such upgraded valve-seat alloys is driven by the demands to meet new emissions and fuel economy goals which continue to push diesel exhaust component temperature higher. Requests for more detailed information on this project should be directed to Caterpillar, Inc.

Approach

Caterpillar will provide and analyze the baseline wear and mechanical behavior characteristics of engine-exposed valves and seats, and similar exposure of those components to laboratory simulation-rig testing at Caterpillar. ORNL will provide more in-depth characterization and microcharacterization of those valves and seats. Data will provide the basis for selecting and testing valve and seat alloys with upgraded performance. Caterpillar and ORNL will work with Caterpillar's various component or materials suppliers so that potential solutions are commercially viable, and so that prototype components are readily available for Caterpillar's test rig or diesel engine evaluation.

Technical Progress – Caterpillar, Inc.

Through their major seat-insert supplier, Caterpillar performed wear resistance evaluations, i.e., a "Plint Wear Test", using the conventional seat-insert material in a pre-oxidized condition with the base valve alloy. Seat insert materials were tested in three different surface oxidation conditions and at three different temperatures. Preliminary fractographic examinations of the wear scars between the tested pin and plate specimens were performed. Additionally, Caterpillar conducted a valve seat insert temperature analysis on valves at three nominal operating temperatures. Knoop microhardness measurements were acquired around the seat insert wear surface in 10 degree increments, at specific depths from the wear surface. Via calibration, hardness measurements were correlated to temperature around the insert wear surface. Caterpillar continued to facilitate dialogue and data exchange between the participants of this project and their major seat-insert supplier.

Technical Progress – ORNL

ORNL conducted microcharacterization studies of valve seat components (non-wear control specimens). Combined SEM and XPS studies of surface oxides and sub-surface regions were completed to benchmark microstructures developed during specific aging schedules. Similar studies will be performed during the next quarter on valve components which have been subjected to specific aging schedules.

Communications/Visits/Travel

Detailed team communications between ORNL and Caterpillar occur regularly in multi-party conference calls. Caterpillar has extended team discussions to include their commercial seat-insert supplier.

Status of Milestones (ORNL for DOE)

New CRADA project that started this quarter.

Publications/Presentations/Awards

None – new CRADA project in FY2008.

Agreement 13329: Mechanical Reliability of PZT Piezo-Stack Actuators for Fuel Injectors

**H.-T. Lin, A. A. Wereszczak, H. Wang and T. A. Cooper
Oak Ridge National Laboratory**

Objective/Scope

Enable confident utilization of piezo stack actuator in fuel injectors for heavy vehicle diesel engines. The use of such actuators in diesel fuel injectors has the potential to reduce injector response time, provide greater precision and control of the fuel injection event, and lessen energy consumption. Though piezoelectric function is the obvious primary function of lead zirconium titanate (PZT) ceramic stacks for fuel injectors, their mechanical reliability can be a performance and life limiter because PZT is brittle, lacks high strength, and is susceptible to fatigue. However, that brittleness, relatively low strength, and fatigue susceptibility can be overcome with the use of appropriate probabilistic design methods.

Technical Highlights

Electric fatigue test under mechanical preload has been conducted on piezo stacks manufactured by Noliac, Denmark. The selected three stack sizes are 5 mm x 5 mm x 18 mm, 5 mm x 5 mm x 10 mm, and 5 mm x 5 mm x 2 mm, and they are designated as A, B, and C, respectively. These piezo stacks are made up of PZT-5A with the Curie temperature 350°C, and are considered to be equivalent to those used in fuel injection system of diesel engines. The new amplifier, Trek PZD350, which can output +/-350 Vpk with +/-200 mA current capability, was used in electric cycling, while another amplifier, Trek 609, was used for evaluations at the specified number of cycles.

The electric fatigue test was initiated and proceeded with size A. The first stack broke down during the pre-fatigue test when semi-bipolar sinusoidal wave was switched from 50 Hz, -60/+200 Vpk to 10 Hz, -60/+300 Vpk. The breakdown mechanism is not clear, but it was suspicious of effect of induced vibration related to the chain that connects the overhead beam and the dead weight [1]. Damping components were then introduced into the upper and lower contact points, which significantly suppressed the vibration. The fatigue test was continued on the second actuator of size A. With the modified contacts, the system managed to finish 100 millions (100M) cycles of semi-bipolar sine wave cycling that had 100 Hz, -60/+300 Vpk with 20 MPa mechanical preload.

Observations showed that discharges occurred during the fatigue test on both electroded lateral faces as that can be evidenced from the dark areas. These dark traces took place either on the interface between two plates or near the solder [Fig. 1(a) and (b)].

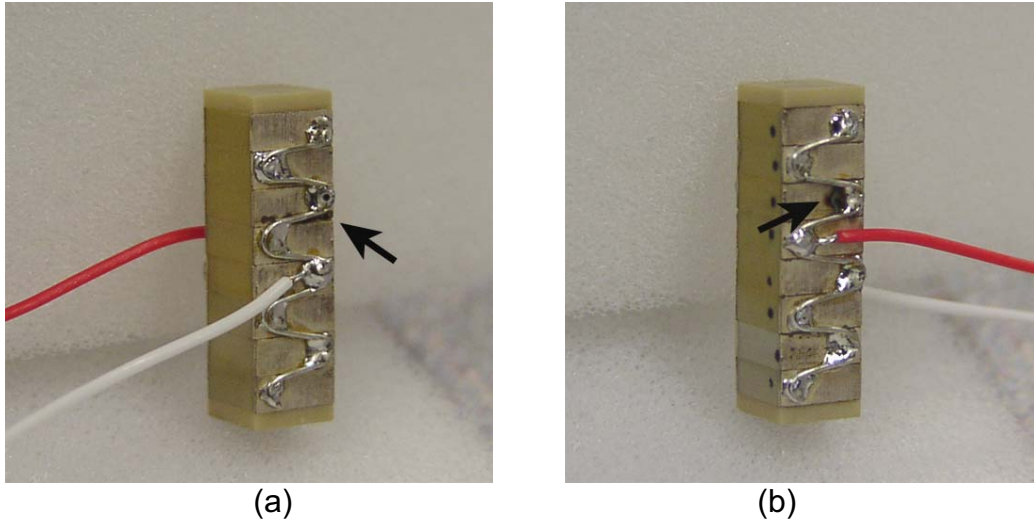
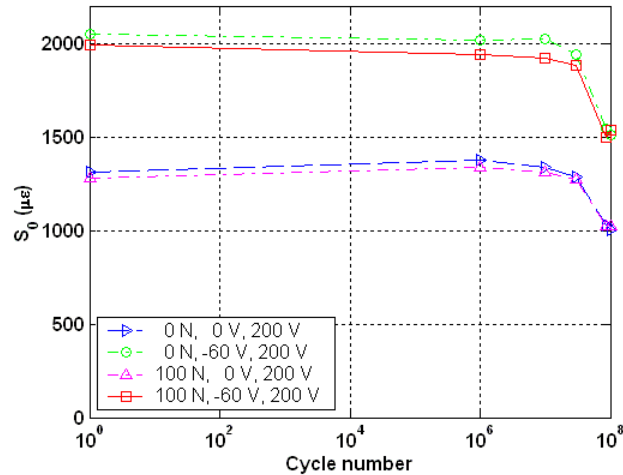


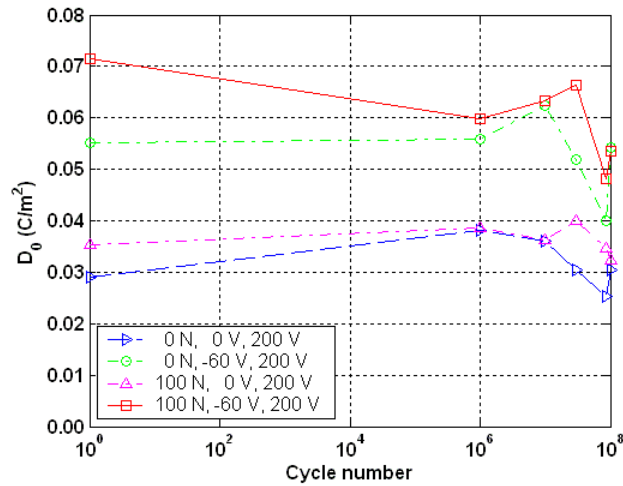
Fig. 1. Photos of #2 size A piezo stack showing the dark traces on the electroded faces whose loading conditions are: 20 MPa mechanical preload, semi-bipolar sine wave with 100 Hz, -60/+300 Vpk, and 100 millions of cycles finished. (a) shows the dark trace near the interface between two plates, and (b) shows the dark trace near the one of solders.

The related response was more sensitive to the negative peak voltage than to the mechanical preload. The reverse electric field raised the mechanical strain and electric charge by more than 50% and 100%, respectively, under the employed measurement condition: 10 Hz, -60/+200 Vpk with 20 MPa preload. Our measurements repeated three times under each electro-mechanical loading condition, and it was found that the mechanical strain appeared to be repeatable but the electric charge density showed sizable variance.

Overall, both the mechanical strain and charge density showed remarkable reduction at the end of 100M cycles. The mechanical strain and the charge density both exhibited about 25% drop under the mentioned measurement condition. These two quantities showed a similar trend of variations under the uni-polar measurement condition: 10 Hz, 0/+200 Vpk, and 20 MPa preload. They exhibited to a certain extent of reduction but with some recovery before the significant drop around 30M cycles. The revealed recovery was also reported in other tests and related mechanism was discussed in [1-3]. Fig.2 (a) and (b) present the fatigue results of the same piezo stack in terms of hysteresis loop amplitude S_0 and D_0 where measuring conditions are given in the legend of respective figures. The preload is given in terms of the dead weight on the beam end, and 0 N and 100 N correspond to 0.7 MPa and 20 MPa, respectively [1]. As it can be seen, 20 MPa preload enhanced electric displacement but not the mechanical displacement; the related mechanism is under investigation.



(a)



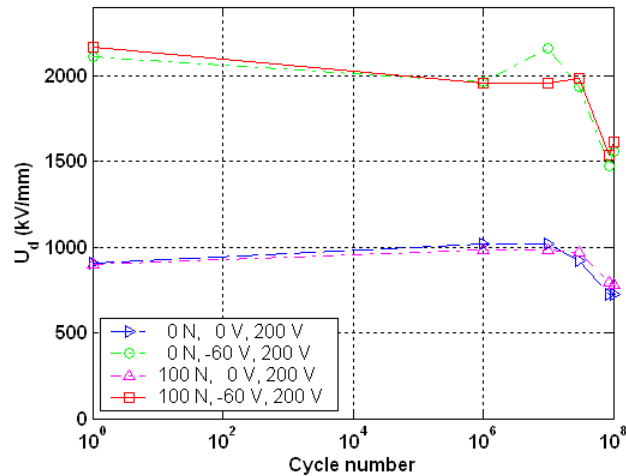
(b)

Fig. 2. Variations of mechanical strain S_0 (a) and charge density D_0 (b) of the same piezo stack as in Fig. 1 during the electric cycling with mechanical preload whose loading conditions are same as given in Fig. 1. The cycling was paused at the designed number of cycles, and measurements were taken under the conditions as given in the legend of respective figures. Each data point is the averaged value of three measurements under same loading condition.

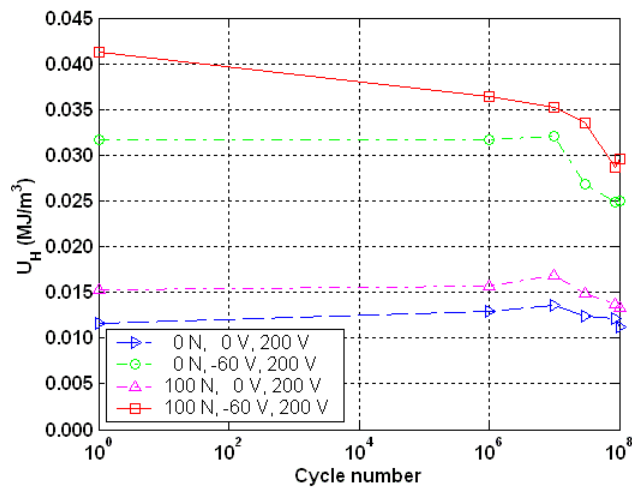
The piezoelectric and dielectric hysteresis exhibited similar degradation patterns and magnitudes to those of the mechanical strain and charge density as it can be seen from Fig. 3(a) and (b). For measures of piezoelectric hysteresis U_d and dielectric hysteresis U_H , please refer to [1]. It, therefore, seems that the domain activity has been reduced significantly by the fatigue.

Components of piezodilatometer have been fabricated and assembled as shown in Fig. 4. Some of these components were modified after receiving from the machine shop, especially insulating ceramic specimen-seat, and high-voltage electrode holder. These modifications are necessary to reduce the risk of possible interaction between the

alumina and the electric fluid as it was found the machine shop had used a low-grade alumina. LABVIEW-based Data acquisition system has been upgraded to accommodate the requirements for the accelerated fatigue testing. Major functions have been implemented.



(a)



(b)

Fig. 3 Variations of hysteresis of the same piezo stack as in Fig.1 and Fig. 2 during the electric cycling with mechanical preload. The cycling was paused at the designed number of cycles, and measurements were taken under the conditions as given in the legend of respective figures. Each data point is the averaged value of three measurements under same loading condition. (a) illustrates the variations of piezoelectric hysteresis U_d and (b) shows those of dielectric hysteresis U_H .

Status of FY 2008 Milestones

Measure and compare reliability of competing commercially available piezoactuators under consideration for use in diesel fuel injectors. [09/08] *On schedule.*

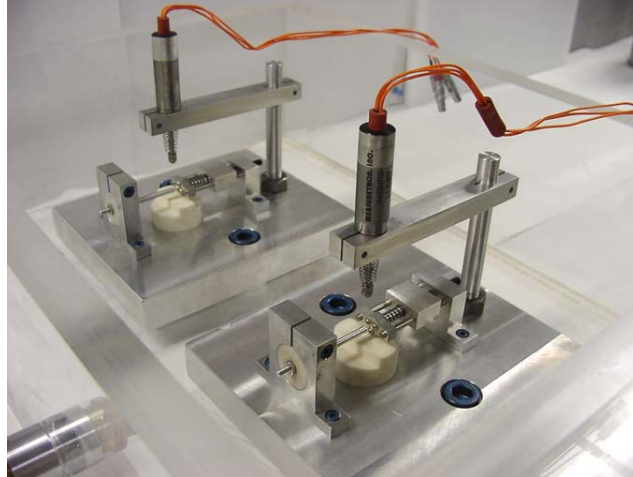


Fig. 4 Photo of the piezodilatometer that has been fabricated, assembled, and ready for calibration. The valve in the lower left is not shown.

Communications/Visits/Travel

Communications were made with Dr. Doug Memering regarding the up-to-date paper work approval status of CRADA on mechanical reliability of PZT actuator.

Publications/Presentations/Awards

1. Wang, H., Wereszczak, A. A., and Lin, H.-T., "Fatigue Response of a PZT Multilayer Actuator Under High-field Electric Cycling with Mechanical Preload," 2008, submitted to *J. Appl. Phys.*
2. Wang, H. and Wereszczak, A. A., "Effects of Electric Field and Biaxial Flexure on the Failure of Poled Lead Zirconate Titanate," *IEEE Trans. Ultrasonic, Ferroelectrics, and Frequency Control*, 2008, in press.

References

1. Wang, H., Wereszczak, A. A., and Lin, H.-T., Fatigue response of a PZT multilayer actuator under high-field electric cycling with mechanical preload, 2008, submitted to *J. Appl. Phys.*
2. Chaplya, P. M., Mitrovic, M., Carman, G. P. and Straub, F. K., Durability properties of piezoelectric stack actuators under combined electromechanical loading, *J. Appl. Phys.*, 100, 124111 (2006)
3. Wang, D., Fotinich, Y. and Carman, G. P., Influence of temperature on the electromechanical and fatigue behavior of piezoelectric ceramics, *J. Appl. Phys.*, 83 (10), 5342-5350 (1998)

Agreement 13332: Friction and Wear Reduction in Diesel Engine Valve Trains

**Peter Blau
Oak Ridge National Laboratory**

Objective/Scope

The objective of this effort is to enable the selection and use of improved materials, surface treatments, and lubricating strategies for valve train components in energy-efficient diesel engines. Depending on engine design and operating conditions, between 5 and 20% of the friction losses in an internal combustion engine are attributable to the rubbing between valve train components. Moreover, wear-induced leaks around valve seats can reduce cylinder pressure and engine efficiency while leading to increased emissions. This effort focuses on understanding the complex wear processes in diesel engine exhaust valves and seats, and applies that knowledge to help engine designers in selecting materials and surface treatments for increased reliability and reduced engine emissions.

FY 2007 witnessed the completion of a high-temperature repetitive impact (HTRI) testing system that is capable of testing the surface durability of candidate exhaust valve materials at diesel engine temperatures. In FY 2008, a three-pronged approach was initiated to investigate the role of wear plus oxidation on the durability of valve material surfaces and apply that understanding to practical engine materials selection. The three prongs are: (1) conducting studies of the effects of surface damage on the growth and repair of oxide scales on contact surfaces exposed to exhaust temperatures, (2) investigating the wear characteristics of selected Fe-, Ni-, and Co-base alloys in the HTRI apparatus built in FY 2007, and (3) developing a multi-component, materials-based model for valve recession that contains the effects of mechanical damage, oxide formation, and adhesive transfer. Information is being shared on a continuing basis with a U.S. diesel engine manufacturer who has also supplied production-grade valves for study.

Technical Highlights

Composition changes in reformed oxides due to abrasion damage. As noted in the last quarterly report, materials used in engine exhaust valves are exposed to a combination of high ambient temperatures, oxidation by hot gases, and mechanical contact that eventually produces surface deformation and wear. During this quarter, experiments continued to investigate whether the oxide that forms on mechanically damaged surfaces of high-temperature alloys, like those used in valves, differs in composition and properties from an oxide that forms on the surface without prior mechanical damage. Three alloys are under investigation: (1) Custom 465, a martensitic Fe-base, age-hardenable alloy; (2) Pyromet 80A, a Ni-based, oxidation resistant alloy; and (3) Stellite 6B, a Co-based, superalloy used for corrosion- and wear-resistance. Compositions and hardness data for these alloys were given in the previous report.

Bruce Pint, leader of the Corrosion Science and Technology Group, studied the oxidation characteristics of the aforementioned alloys using a micro-gravimetric (weight gain) technique. Specimens were exposed to oxygen at 850°C for 25 hours, and results are summarized in Figure 1. The behavior of the Stellite 6B and the Pyromet 80A was

similar, but the Custom 465, an Fe-based alloy, experienced a significant change in the oxidation rate after an incubation period of about an hour. Based on these results, it was of interest to determine whether there would be also a difference in the oxides if mechanical damage were present on the surfaces.

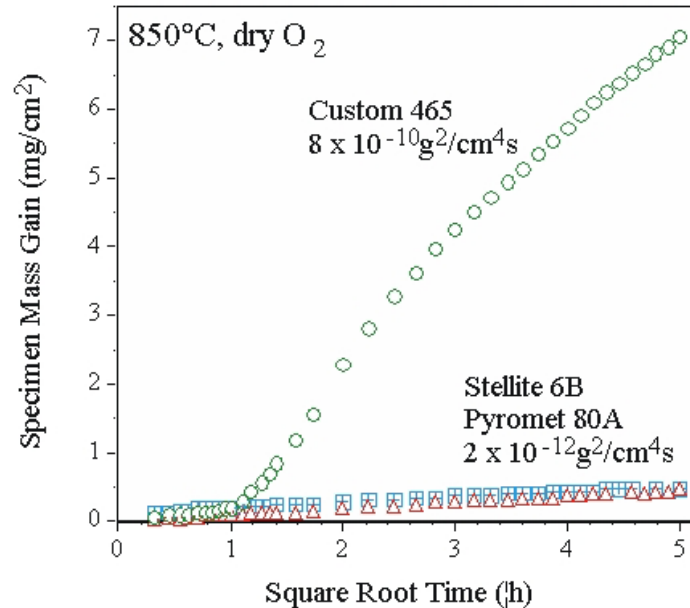


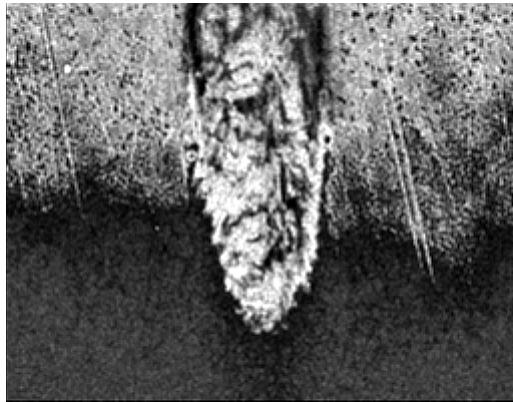
Figure 1. Oxidation of three alloys at 850°C in oxygen

Polished surfaces of the three alloys were oxidized for two hours at 850°C, a surface temperature typical of some diesel engine exhaust valves and the same temperature for which the aforementioned oxidation data were obtained. Then scratches were made on the scale-covered surfaces and the coupons were replaced into the furnace for another four hours.

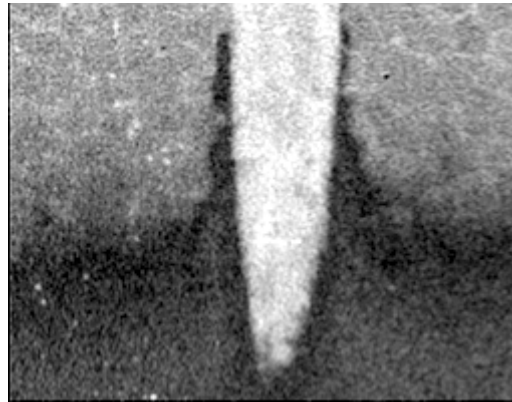
A special metallographic technique, called taper-polishing, was used to reveal the structure of the scratch damage as well as the adjacent oxide scales. By placing these taper sections in a scanning electron microscope equipped for energy-dispersive analysis (JEOL 3400), X-ray composition maps of the surfaces of scratched and re-oxidized surfaces were captured. The assistance of Tracie Brummett in performing the EDX analysis is acknowledged. Images showed significant differences in the elemental distribution on and off the scratched and re-oxidized areas. For example, differences between the chromium (Cr) content on and off the scratches that were re-oxidized are displayed for all three alloys in Figures 2 (a), (b), and (c), respectively. The brighter the area, the higher is the Cr content in this case. Clearly, the intensity of the Cr signal is quite different in the centers of the scratches and on the oxide that formed on the surface to the sides of the scratches. Furthermore, in Figure 2(b) the Cr is seen to concentrate in chromium carbides rather than be more uniformly distributed, as in the case of the other alloys.

Elemental maps of other species like Fe, Co, Ni, Al, O, and Ti were also obtained and showed compositional differences as well. It is evident from these results that abrasion

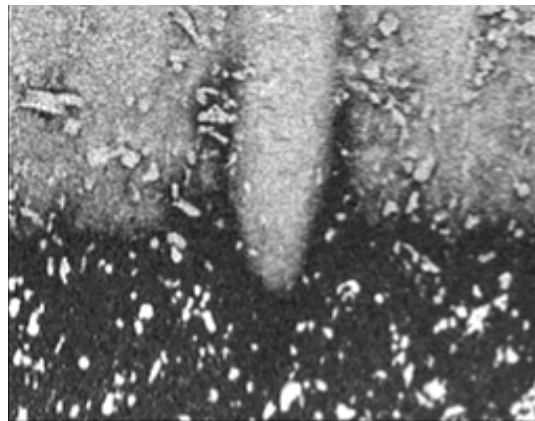
and, most likely, other forms of surface damage can affect the subsequent formation of oxides on valve materials. Therefore, static corrosion data, that is, data obtained without mechanical contact, cannot be used to directly predict the durability of valve materials. Two papers are being prepared to detail these results. One has been submitted to an international tribology journal and the other to an upcoming conference on the wear of materials (see below for details).



(a) Custom 465



(b) Pyromet 80A



(c) Stellite 6B

Figure 2. X-ray maps show the distribution of chromium in taper cross-sections of the surfaces of alloys that were scratched and re-oxidized at 850°C. (*Note: Due to the 5 degree tilt of the taper polish, the dimensions of features the vertical direction are effectively enlarged by a factor of 10.*)

Future Plans

1) Complete high-temperature repetitive impact tests on the candidate alloys and prepare a final report.

Travel

P. Blau attended the Annual Meeting of the Society of Tribologists and Lubrication Engineers (STLE), Cleveland, Ohio, May 5-8, 2008, and participated as an invited panelist in a discussion of the mechanisms and analysis of scuffing damage in materials (see the presentation list, below).

Status of Milestones

- 1) Complete experiments on the effects of surface damage on oxide formation and prepare a paper for journal submission. **(6/08 - completed)**
- 2) Submit a final report that summarizes wear studies on candidate valve materials and presents a model for valve seat recession. **(09/08)**

Publications and Presentations

P. J. Blau, "The Many Faces of Scuffing: Mechanisms, Measurements, and Control," presentation and panel discussion, 2008 Annual Meeting of the Society of Tribologists and Lubrication Engineers (STLE), Cleveland, Ohio, May 8, 2008.

P. J. Blau and T. M. Brummett, "High-Temperature Oxide Regrowth on Mechanically-Damaged Surfaces", submitted to *Tribology Letters*.

P. J. Blau, T. M. Brummett, and B.A. Pint, "Effects of prior surface damage on high-temperature oxidation of Fe-, Ni-, and Co-based alloys," submitted to the 2009 International Conference on Wear of Materials, Las Vegas, Nevada, April 19-22; also for publication in the journal *Wear*.

Agreement 9089: NDE of Diesel Engine Components

J. G. Sun and J. A. Jensen*
Argonne National Laboratory

***Caterpillar, Inc.**
Technical Center

Objective/Scope

Emission reduction in diesel engines designated to burn fuels from several sources has led to the need to assess ceramic valves to reduce corrosion and emission. The objective of this work is to evaluate several nondestructive evaluation (NDE) methods to detect defect/damage in structural ceramic valves for diesel engines. One primary NDE method to be addressed is elastic optical scattering. The end target is to demonstrate that NDE data can be correlated to material damage as well as used to predict material microstructural and mechanical properties. There are two tasks to be carried out: (1) Characterize subsurface defects and machining damage in flexure-bar specimens of NT551 and SN235 silicon nitrides (Si_3N_4) to be used as valve materials. Laser-scattering studies will be conducted at various wavelengths using a He-Ne laser and a tunable-wavelength solid-state laser to optimize detection sensitivity. NDE studies will be coupled with examination of surface/subsurface microstructure and fracture surface to determine defect/damage depth and fracture origin. NDE data will also be correlated with mechanical properties. (2) Assess and evaluate surface and subsurface damage in Si_3N_4 and TiAl valves to be tested in a bench rig and in an engine. All valves will be examined at ANL prior to test, during periodic scheduled shut downs, and at the end of the planned test runs.

Technical Highlights

Work during this period (April-June 2008) focused on evaluating various NDE technologies developed at ANL for applications in material/component developments for high-efficiency diesel engines.

1. Laser-Scatter NDE Evaluation of Engine-Tested Valves

Ten Si_3N_4 engine valves, which were used in engine duration test at ORNL for up to 555 hours, were inspected at ANL in early FY2008 using the laser-backscatter valve-scan system. These valves were then machined into half-cylinder specimens and fracture tested at ORNL. The availability of destructive test results (strength) and NDE data for these specimens presents a unique opportunity for correlating the NDE data with destructive test results. During this period we have received these specimens from Dr. H.-T. Lin of ORNL. Figure 1 shows a photograph of a set of fractured specimens from the stem of exhaust valve #21. The valve stem has produced 4 fracture-test specimens, each exhibits one or two fractures from the destructive test. The laser-scatter NDE image for this stem is shown in Fig. 2, acquired in FY2007. The scan image has a pixel size (or spatial resolution) of $10\mu\text{m}$, which is sufficient to detect material inherent defects (pores with sizes up to $70\mu\text{m}$) and damages such as indents or scratches. The fractured specimens are being examined to determine the location of fracture initiation defect/damage, which is likely near surface and therefore has been

detected in the NDE image. The fracture initiation defect/damage will then be located in the NDE image to determine its type, size, and geometry. The NDE data may therefore help to understand the fracture mechanism and to establish correlation between material's mechanical property and microstructural flaw distribution.



Fig. 1. Photograph of fractured specimens produced from the stem of Si₃N₄ exhaust valve #21.

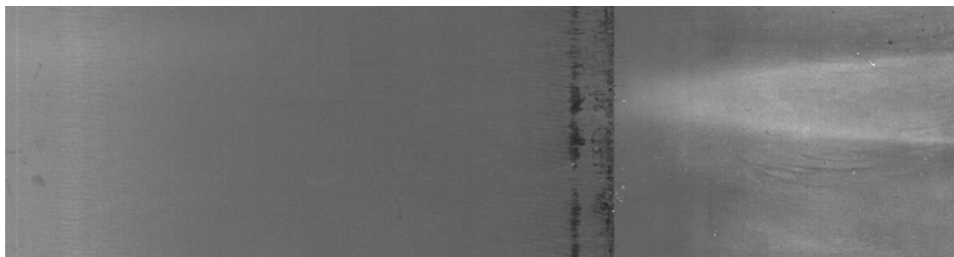


Fig. 2. Laser-scatter scan image for the stem of exhaust valve #21 at end of engine test.

2. NDE Inspection of Joints

During this period we have also received two TiAl wheel specimens from Dr. Y. Nan of Caterpillar, Inc. The wheels were jointed to shafts by high-speed friction joining process. To ensure the joining quality and facilitate the process development, NDE becomes necessary to detect and characterize flaws that may present in the joint. For such application, ultrasonic methods are usually used because they have high sensitivity in detecting poor and weak joints. However, because of the complex geometry of the joint, it may become challenging to interpret “flaws” once they are found and to understand their effect to the joint quality. Therefore, in addition to investigate ultrasonic methods, imaging technologies such as x-ray imaging and thermography are also been explored for NDE characterization of these joints to obtain visual observation of the flaw geometry. Preliminary radiography results using a 420kVp x-ray source indicated that the joining is generally tight at OD but maybe weak at ID. These results are being further evaluated and will be presented in the next report.

3. NDE Technologies to Be Evaluated for Engine Materials/Components Studies

Several NDE technologies developed at ANL are being evaluated for application to high-efficiency diesel engine materials and components. They include thermal imaging methods capable for quantitative measurement of thermal properties for single and multiple layer materials including coatings, and ultrasonic Rayleigh wave method based

on phased array and optical backscatter method based on fiber array for high-speed inspection of surface/subsurface flaws in (ceramic) bearing balls (or other complex-shape components). These technologies are briefly described below.

Thermal Imaging Methods

Thermal imaging involves with the generation and detection of a thermal signature from specimen surfaces. Among the various modes of thermal imaging practices, ANL has focused on vibrothermography and pulsed thermal imaging technologies. In vibrothermography, a vibration (typically ultrasonic) excitation is applied on a specimen to generate frictional heating from cracks (flaws) on or near surface that can be detected by an infrared camera. This technology is effective to detect fatigue cracks and other types of material damages and is being actively studied at present. A major effort at ANL however has been on developing new methods based on pulsed thermal imaging technology. These methods may measure thermal properties (conductivity and diffusivity) of single and multilayer (e.g., coatings) materials, detect vertical and lateral cracks (e.g., cracks in joint; debond in multilayer structure), and determine the depth of flaws under surface. Recently a new thermal tomography method was developed and was granted a US patent in this period. It can construct 3D images (similar to 3D CT data) of material's thermal effusivity in an entire specimen volume. Figure 3 shows typical results for a ceramic-composite plate of 2.5-mm thick with 7 flat-bottom holes machined from the back surface (the hidden surface): one plane effusivity image at 1.2mm deep (left) and two cross-section effusivity images (middle) with corresponding material diagrams (right) along the two lines marked in the plane image. All flat-bottom holes and many smaller defects (darker spots) are resolved in these images.

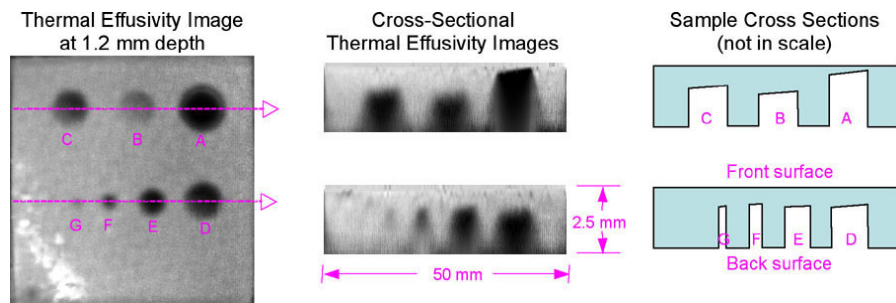


Fig. 3. Typical thermal tomography images for a ceramic plate with flat-bottom holes machined at back surface.

Ultrasonic Rayleigh Wave Method Based on Phased Array

Ultrasonic Rayleigh waves are widely used for detecting near surface features because the energy of the waveform is concentrated within a shallow surface layer. It has been investigated at ANL for high-speed inspection of ceramic bearing balls. To increase the detection sensitivity, ANL developed a specialized phased-array system for generation and detection of Rayleigh waves. In this system, the waves from all array elements are superimposed to produce a stronger Rayleigh wave, resulting in higher detection sensitivity. The ANL phased-array system is shown in Fig. 4. Figure 5 is a scan result

for a ceramic ball surface; it displays the sensitivity for detecting a crack as a function of distance; note that the crack can be detected up to a distance of >25mm from the point where Rayleigh wave is initiated.

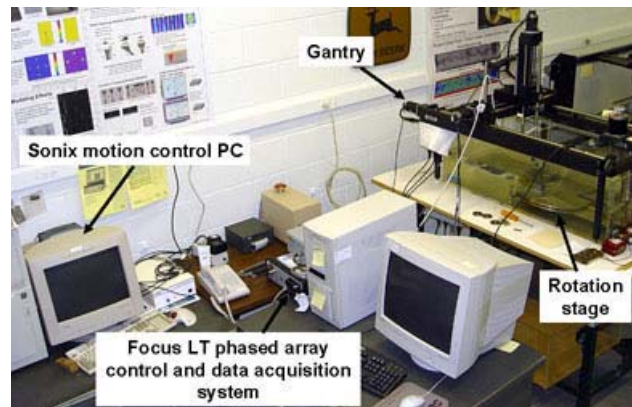


Fig. 4. Photograph of ultrasonic phased-array scanning system at ANL.

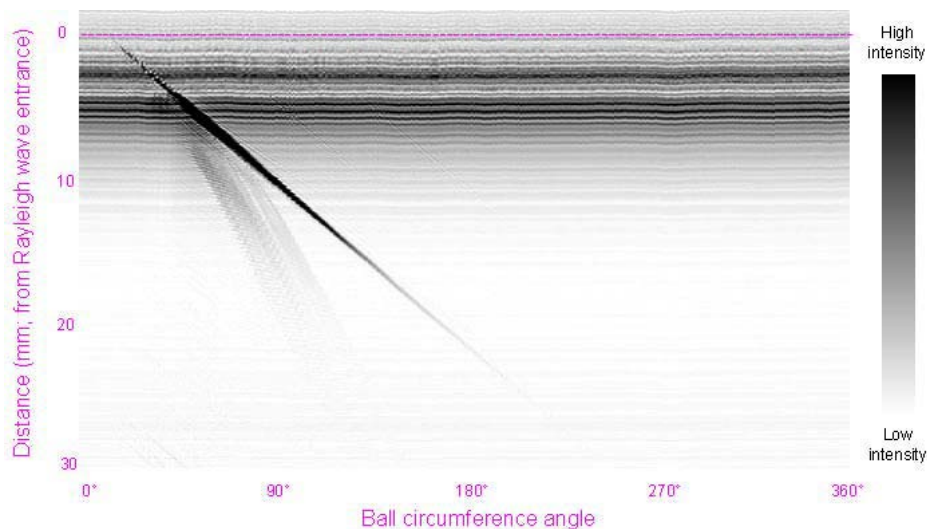


Fig. 5. Rayleigh wave detection sensitivity for a crack as a function of crack distance.

Optical Backscatter Method Based on Fiber Array

For high-speed inspection of complex geometry specimens, such as bearing balls, ANL developed an optical backscatter technology based on optical fiber arrays. By placing optical fibers in an array that closely match the specimen geometry, data from an entire surface could be obtained in a 1D scan (instead of a 2D scan). Figure 6 shows a photograph of a fiber array fabricated from fibers of 250 μm in diameter. The light was transmitted to the specimen (ball) surface by one set of fibers, and the reflected light was detected by another set of adjacent fibers. Figure 7 shows a typical data obtained from an automated scan of a metal bearing ball. In this case, on the surface of the ball were written a set of numerals that were faithfully reproduced in the scan image. Our current system uses a fiber-array probe fabricated from 50- μm -diameter fibers to achieve a higher spatial resolution.



Fig. 6. Photograph of a fiber-array probe and a bearing ball for laser backscatter experiments.

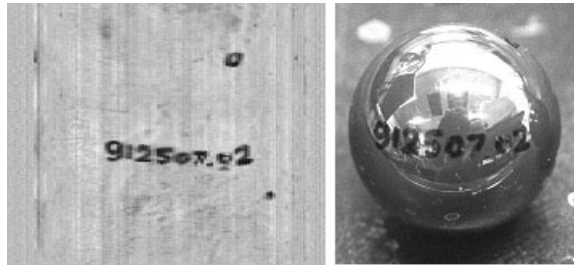


Fig. 7. Laser backscatter scan data (left) from a 25-mm-diameter bearing ball (right) obtained with the optical fiber array shown in Fig. 6.

Status of Milestones

Current ANL milestones are on schedule.

Communications/Visits/Travel

None this period.

Problems Encountered

None this period.

Publications

J.G. Sun, "Method for Thermal Tomography of Thermal Effusivity from Pulsed Thermal Imaging," U.S. Patent No. 7,365,330, issued April 29, 2008.

**Agreement 9130: Development of Materials Analysis Tools
for Studying SCR Catalysts**

**Thomas Watkins, Larry Allard, Michael Lance and Harry Meyer
Oak Ridge National Laboratory**

**Krishna Kamasamudram, Cheryl Klepser and Alex Yezerets
Cummins Inc.**

Objective

The objective of this effort is to produce a quantitative understanding of the interdependence between structure and performance to develop options for an exhaust after treatment system with improved final product performance in order to meet the US Environmental Protection Agency emissions requirements for 2010 and beyond.

Technical Progress

A commercial Fe-zeolite powder was hydrothermally aged at 500, 700, and 900°C for 12 hours at a space velocity of 40000 lit/lit/h. The atmosphere will be 10% H₂O, 18% O₂ and 72% N₂. Catalyst characterizations (X-ray diffraction, transmission electron microscopy, X-ray photoelectron spectroscopy, Raman Spectroscopy) are in progress.

Agreement 10461: Durability and Reliability of Ceramic Substrates for Diesel Particulate Filters

Amit Shyam, Thomas R. Watkins and Edgar Lara-Curzio
Oak Ridge National Laboratory

Objectives/Scope

To develop/implement test methods to characterize the physical and mechanical properties of ceramic diesel particulate filters (DPFs), and to implement a probabilistic-based analysis to quantify their durability and reliability.

Highlights

- The microstructural characteristics of a field returned diesel particulate filter (135,000 miles) was characterized.
- The thermal expansion and mechanical behavior of field returned diesel particulate filter was related to the microstructure of the material.

Technical Progress

The mechanical reliability of engineering systems is determined by the intersection region between the distributions of mechanical strength and service stress. DPFs fabricated from porous cordierite have a complex microstructure with microcracks that can heal themselves during high temperature operation and reopen during subsequent cooling. This microstructural phenomenon makes the mechanical properties of the DPF a dynamic property which can change as a result of the operating service history. It is therefore, of interest to characterize the mechanical and thermal shock characteristics of filters that have been returned from field service in order to refine the lifetime prediction procedure for DPFs. The results from the thermal and mechanical characterization of soot loaded high mileage filters were reported in the previous quarter. The microstructural aspects of soot loaded filter materials and the relevant microstructure-mechanical properties are identified and reported. The high mileage filter was sectioned in half and characterized by Cummins via time-of-flight ultrasound techniques and the results are shown in Figure 1. As reported in the previous quarter, specimens for mechanical and thermal expansion evaluation were evaluated from two different regions of the filter. These regions are labeled C13 and C19 in Figure 1 and represent the core and peripheral regions of the filter, respectively.

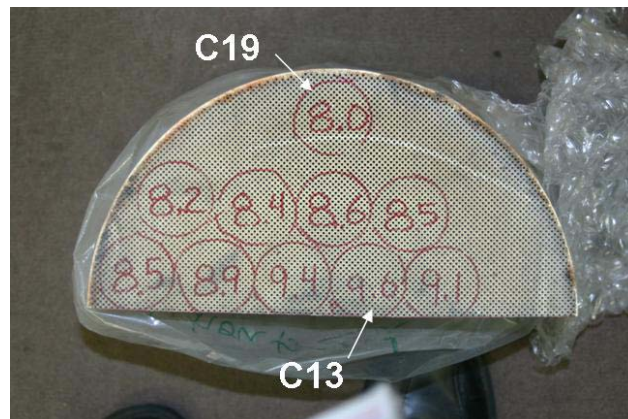


Figure 1. The half-cross section of a high mileage DPF.

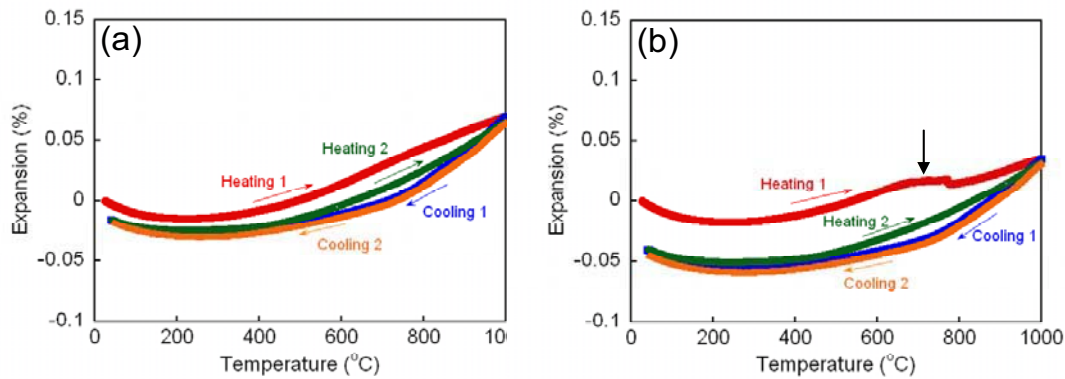


Figure 2. Comparison of the thermal expansion behavior of specimens from different regions of a high mileage filter (a) C13 – core region and (b) C19 – peripheral region. The direction of expansion is parallel to the extrusion direction and information for two heating and cooling cycles is included.

The thermal expansion behavior parallel to the extrusion direction for specimens prepared from the high mileage filter is shown in Figure 2. Figures 2(a) and (b) represent the behavior of test specimens prepared from the core (C13) and peripheral (C19) regions of the filter, respectively. The shape of the thermal expansion curves in Figure 2 is similar to what has been reported previously for virgin cordierite. Thermal expansion in the peripheral region, however, leads to an extended plateau (shown with an arrow in Figure 2(b)) in the temperature range of 600 to 800°C.

It was reported in the previous quarter that the high mileage filter specimens had a higher fracture toughness compared to specimens from the virgin uncoated and unexposed filter. C13 (core) and C19 (periphery) region specimens had a fracture toughness of 0.35 ± 0.03 and 0.40 ± 0.02 MPa \sqrt{m} , respectively. This is compared to virgin specimens that had an average fracture toughness of 0.32 ± 0.04 MPa \sqrt{m} . The increase in fracture toughness due to service conditions can be partially explained by the scanning electron micrographs (SEM) in Figure 3. Figures 3 (a) and (c) are images of the microstructure of C13 (core) region and should be compared with the microstructure of the virgin specimen in Figures 3 (b) and (d), respectively. It may be concluded from Figure 3 that the soot particles (bright regions) can have a consolidating effect on the pores and can therefore, help increase the fracture toughness of specimens that have been through service conditions. The elevated temperature service conditions can also lead to permanent healing of microcracks in the microstructure but detailed quantitative microcrack density measurements have not been performed at this time.

An SEM image of the microstructure of a specimen from the peripheral region of the filter is shown in Figure 4. Specimens from the outer region have higher levels of soot loading compared to specimens from the core region consistent with higher temperatures in the core region of the filter that can lead to a larger fraction of the soot particles burning out. This observation can be related to the extended plateau (Figure 2(b)) in the thermal expansion curve of the specimens from the peripheral region of the high mileage filter. The plateau could be an artifact from the soot burning process since it is absent in the second heating cycle.

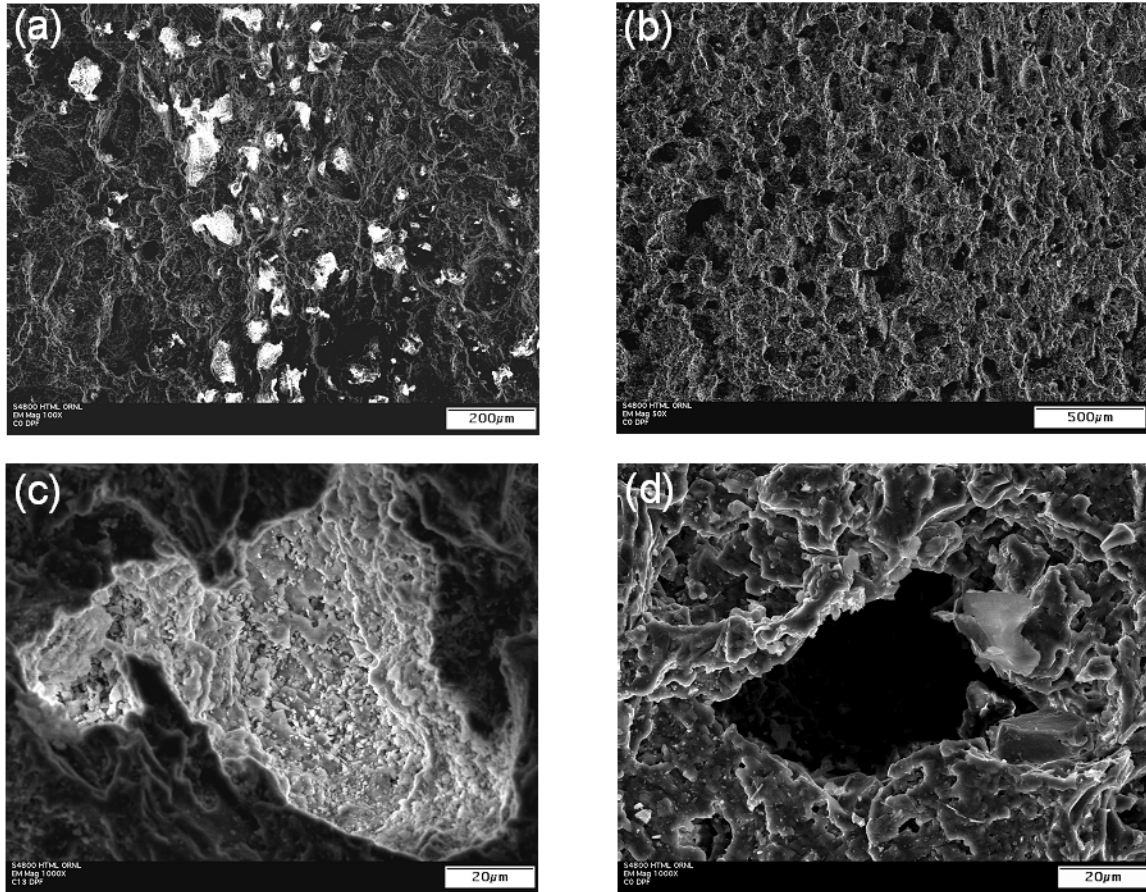


Figure 3. SEM images showing a comparison of the microstructure of the high mileage filter (C13) with the virgin uncoated material. (a) and (b) are comparisons at low magnification with the bright regions in (a) representing soot and (c) pore filled with soot (d) pore at the same magnification in the virgin material.

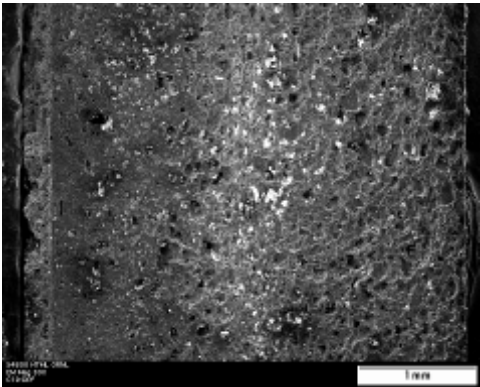


Figure 4. SEM image with microstructure of a specimen from the peripheral region (C19) of the as-received high mileage filter.

Other activities that were initiated in this quarter were characterization of the porosity of the specimens as a function of thickness and *in-situ* observation of filter microstructure in a high temperature SEM stage. These will be reported in the future.

Publications

Amit Shyam, Edgar Lara-Curzio, Thomas R. Watkins and Randy J. Parten, "Mechanical characterization of diesel particulate filter (DPF) substrates" *Journal of the American Ceramic Society*, vol. 91, no. 6, pp. 1995-2001, June 2008.

Meetings

Randy Stafford from Cummins Inc. visited ORNL and discussed the CRADA with team members in August 2008.

Agreement 10635: Catalysis by First Principles - Can Theoretical Modeling and Experiments Play a Complimentary Role in Catalysis?

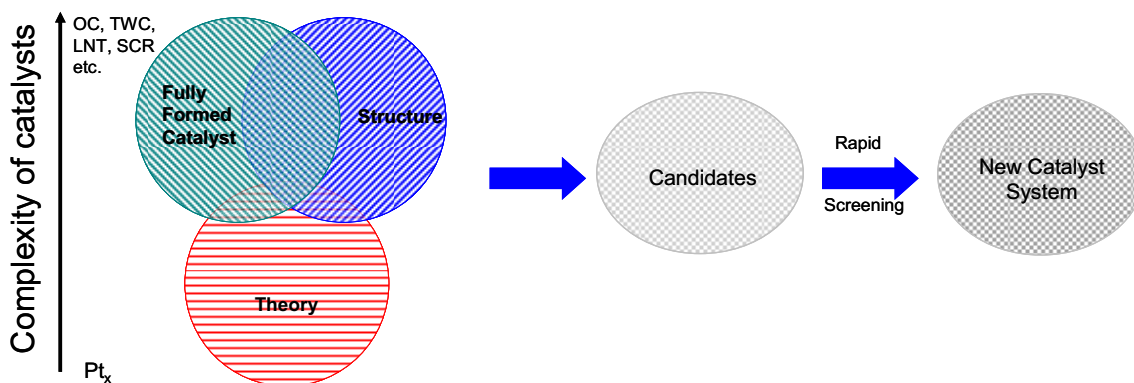
**C. Narula, M. Moses, and L. Allard
Oak Ridge National Laboratory**

Objective/Scope

This research focuses on an integrated approach between computational modeling and experimental development, design and testing of new catalyst materials, that we believe will rapidly identify the key physiochemical parameters necessary for improving the catalytic efficiency of these materials. The results will have direct impact on the optimal design, performance, and durability of supported catalysts employed in emission treatment; e.g., lean NO_x catalyst, three-way catalysts, oxidation catalysts, and lean NO_x traps etc.

The typical solid catalyst consists of nano-particles on porous supports. The development of new catalytic materials is still dominated by trial and error methods, even though the experimental and theoretical bases for their characterization have improved dramatically in recent years. Although it has been successful, the empirical development of catalytic materials is time consuming and expensive and brings no guarantees of success. Part of the difficulty is that most catalytic materials are highly non-uniform and complex, and most characterization methods provide only average structural data. Now, with improved capabilities for synthesis of nearly uniform catalysts, which offer the prospects of high selectivity as well as susceptibility to incisive characterization combined with state-of-the science characterization methods, including those that allow imaging of individual catalytic sites, we have compelling opportunity to markedly accelerate the advancement of the science and technology of catalysis.

Computational approaches, on the other hand, have been limited to examining processes and phenomena using models that had been much simplified in comparison to real materials. This limitation was mainly a consequence of limitations in computer hardware and in the development of sophisticated algorithms that are computationally efficient. In particular, experimental catalysis has not benefited from the recent advances in high performance computing that enables more realistic simulations (empirical and first-principles) of large ensemble atoms including the local environment of a catalyst site in heterogeneous catalysis. These types of simulations, when combined with incisive microscopic and spectroscopic characterization of catalysts, can lead to a much deeper understanding of the reaction chemistry that is difficult to decipher from experimental work alone.



Thus, a protocol to systematically find the optimum catalyst can be developed that combines the power of theory and experiment for atomistic design of catalytically active sites and can translate the fundamental insights gained directly to a complete catalyst system that can be technically deployed.

Although it is beyond doubt computationally challenging, the study of surface, nanometer-sized, metal clusters may be accomplished by merging state-of-the-art, density-functional-based, electronic-structure techniques and molecular-dynamic techniques. These techniques provide accurate energetics, force, and electronic information. Theoretical work must be based on electronic-structure methods, as opposed to more empirical-based techniques, so as to provide realistic energetics and direct electronic information.

A computationally complex system, in principle, will be a model of a simple catalyst that can be synthesized and evaluated in the laboratory. It is important to point out that such a system for experimentalist will be an idealized simple model catalyst system that will probably model a “real-world” catalyst. Thus it is conceivable that “computationally complex but experimentally simple” systems can be examined by both theoretical models and experimental work to forecast improvements in catalyst systems.

Our Goals are as follows:

- Our theoretical goal is to carry out the calculation and simulation of realistic Pt nanoparticle systems (i.e., those equivalent to experiment), in particular by addressing the issues of complex cluster geometries on local bonding effects that determine reactivity. As such, we expect in combination with experiment to identify relevant clusters, and to determine the electronic properties of these clusters.
- Our experimental goal is to synthesize metal carbonyl clusters, decarbonylated metal clusters, sub-nanometer metal particles, and metallic particles (~5 nm) on alumina (commercial high surface area, sol-gel processed, and mesoporous molecular sieve), characterize them employing modern techniques including Aberration Corrected Electron Microscope (ACEM), and evaluate their CO, NO_x, and HC oxidation activity.

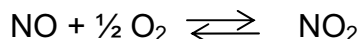
- This approach will allow us to identify the catalyst sites that are responsible for CO, NO_x, and HC oxidation. We will then address support-cluster interaction and design of new durable catalysts systems that can withstand the prolonged operations.

Technical Highlights

Our results on experimental studies of Platinum-Alumina Systems and their nanostructural changes under NO-oxidation conditions are summarized in the following paragraphs. We have initiated our study of nanostructural changes in this catalyst system during hydrocarbon oxidation also.

Experimental Studies

NO Oxidation: 1 nm 2%Pt/γ-Al₂O₃ catalyst, prepared by the traditional impregnation method from H₂PtCl₆ • xH₂O, was exposed to NO oxidation conditions at a space velocity of 50,000 h⁻¹. The concentrations of NO and NO_x during 2 cycles of NO oxidation were monitored every 50°C from 100-650°C, see Figure 1. In the first cycle, oxidation initiated at ~250°C; however, during the second cycle, initiation of NO oxidation was observed at ~150°C. NO oxidation peaked in both cycles at 400°C after which the reverse NO₂ reduction reaction, see eq. 1, dominated through the end of testing at 650°C.



Eq. 1

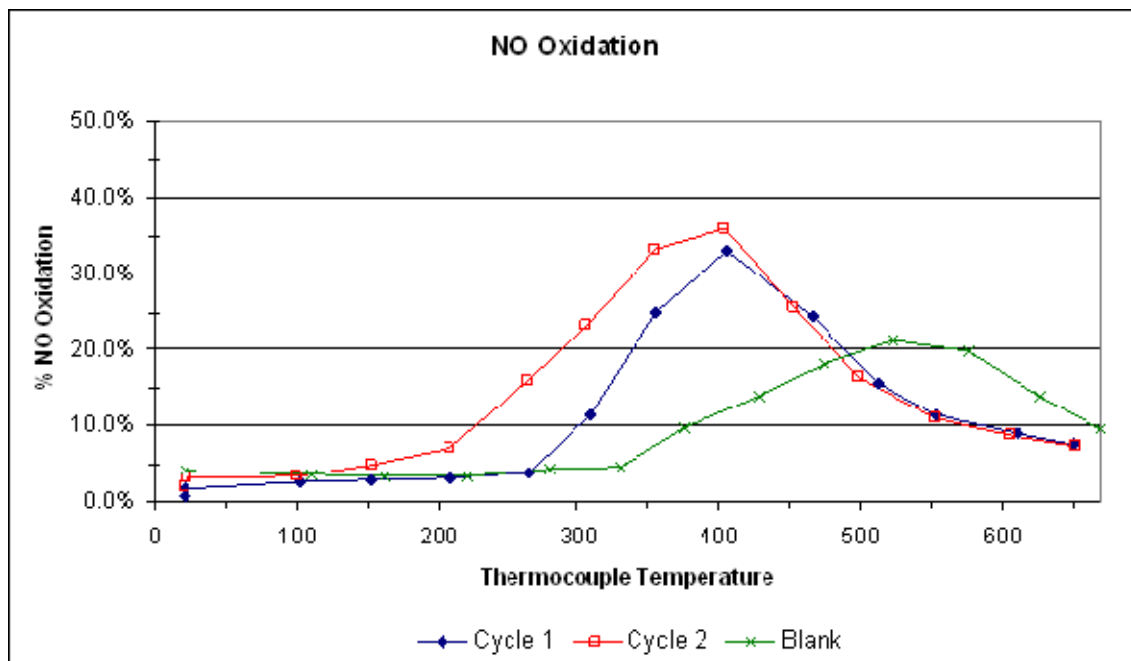


Figure 1. Percentage of NO oxidation as a function of time over a 1 nm 2%Pt/γ-Al₂O₃ catalyst for 2 cycles and blank cycles run without a catalyst sample.

The incomplete oxidation of NO on Pt nanoparticles is not surprising. It is explained by our previously reported theoretical studies which suggest that the ability of the Pt nanoclusters to catalyze NO oxidation may be inhibited by the strongly adsorbed NO. Because of the smaller enthalpy of the overall reaction $\text{NO}(\text{g}) + \frac{1}{2}\text{O}_2(\text{g}) \rightarrow \text{NO}_2(\text{g})$, the somewhat more strongly adsorbed O atom diminishes the energetic driving force for $\text{Pt}_x\text{-O} + \text{NO}(\text{g}) \rightarrow \text{NO}_2(\text{g})$ and makes the Pt_x clusters insufficient oxidizers for NO oxidation.

Figure 2 shows the particles size distribution comparison to starting material (fresh 1nm Pt) which highlights the significant sintering that occurred. A comparison with fresh 1nm Pt catalyst that has been annealed at 650°C/5hrs and has Pt particles of ~12nm suggests that the large particles observed after 2 cycles to 650°C during the NO oxidation were likely a result of the elevated temperatures rather than the NO oxidation environment.

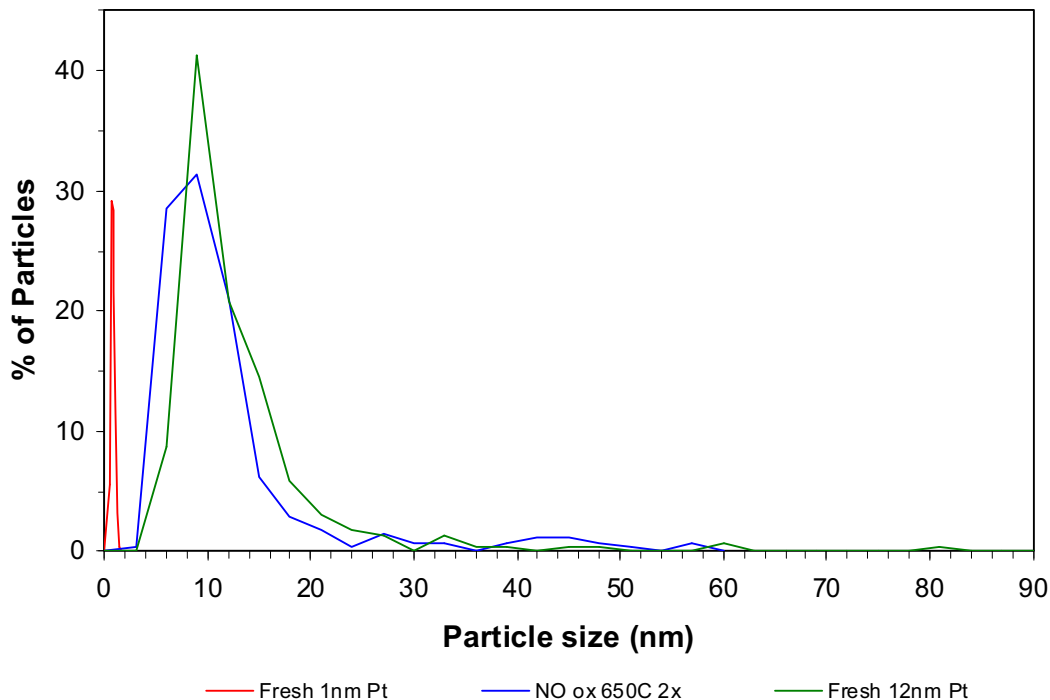


Figure 2. Particle size distribution of fresh 1 nm 2%Pt/ γ -Al₂O₃, after 2 cycles of NO oxidation up to 650°C and fresh 12 nm 2%Pt/ γ -Al₂O₃ catalyst.

In order to better follow and understand the microstructural changes that occur as a result of NO oxidation, we have initiated an ex-situ study. In this study we followed an area of 2%Pt/ γ -Al₂O₃ from fresh through cycles of NO oxidation to observe how the same exact area changes. Since oxidation is only favored up to 400°C, we are only

exposing the sample to NO oxidation conditions up to 450°C which is also the maximum temperature to which a diesel emission catalyst is typically exposed .

An area of fresh 2%Pt/ γ -Al₂O₃ catalyst, see Figure 3, that had Pt particles ranging from 0.7 to 1.7nm with an average size of 1.1nm was exposed to 1 cycle of NO oxidation conditions (10%O₂/ 500ppm NO/ N₂ balance) up to 450°C. When the same area was imaged after the 1 cycle exposure, the Pt particles ranged in size from 0.7 to 4.6nm and had an average size of 1.4nm, see Figure 3.

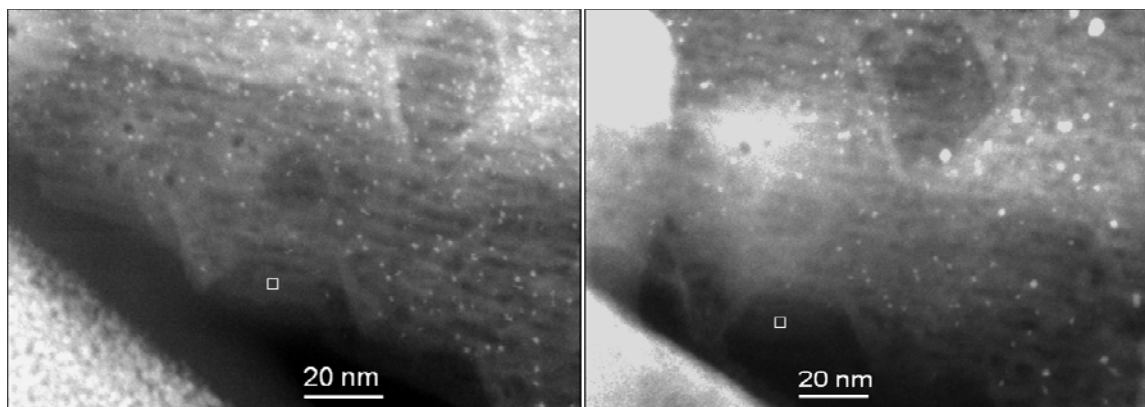


Figure 3. DF-STEM images of 2%Pt/ γ -Al₂O₃ fresh (left) and the exact same area after 1 cycle of NO oxidation to 450°C (right). The white square is located in the same spot on each image to help show comparison.

Figure 4 compares the particle size distribution curve for the fresh and 1 cycle aged sample. The curve for the sample after 1 cycle of aging closely matches the fresh image except that it tails out to a high size range. This result also supports an earlier assertion that the dramatically larger Pt sizes imaged after exposure to 2 cycles of NO oxidation at temperatures up to 650°C (Figure 2) are a product of the high temperature exposure and not the NO oxidation environment. Further, ex-situ tests on NO oxidation effect on Pt particles' microstructure are on-going.

Comparison of Fresh 1 nm 2%Pt/ γ -Al₂O₃ and After 1 Cycle of NO ox up to 450°C

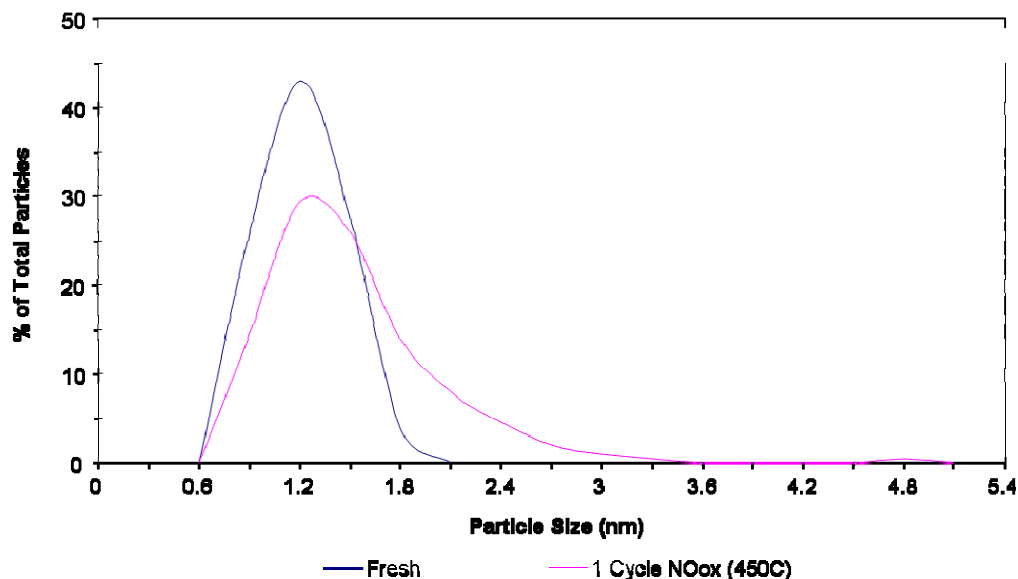


Figure 4. Particle size distribution curves for the exact same area of fresh 2%Pt/ γ -Al₂O₃ and after 1 cycle of NO oxidation to 450°C. These distributions correspond to the images seen in Figure 3.

Next Steps

We plan to carry out the following tasks:

- We will carry out NO_x and HC oxidation on catalyst and monitor nanostructural changes in catalyst samples. We will also correlate the results with theoretical studies.
- We will continue to investigate the thermal chemistry of CO and NO oxidation on free Pt and Pt oxide clusters as well as the properties of Pt and Pt oxide clusters supported on metal oxides (include magnesia and alumina). These investigations will help us gain a better understanding of the structural and catalytic properties of the supported Pt clusters and identify the effect of the support on these important properties.

Barriers/Difficulties

The TEM instrument has been under constant repair making it difficult to analyze samples and carry out ex-situ reactor studies.

Other Activities

A joint project on lean NO_x treatment is on going with John Deere Co. under work for others arrangement. A new work for other arrangement is in process to improve thermal durability of NO_x catalysts with C3 International.

Communication/Visitors/Travel

C.K. Narula will present a poster titled "Catalyst by Design - Bridging the Gap between Theory and Experiments at nanoscale level" at DEER 2008, August 4-7, Dearborn, MI.

Publications

1. C.K. Narula, "Catalyst by Design – Bridging the Gap between Theory and Experiments at Nanoscale Level" Encyclopedia of Nanoscience and Nanotechnology, Taylor & Francis, New York, 2008 (in press).
2. C.K. Narula, L.F. Allard, D.A. Blom, M. Moses-DeBusk, "Bridging the Gap between Theory and Experiments – Nano-structural Changes in Supported Catalysts under Operating Conditions" SAE-2008-01-0416.
3. C.K. Narula, L.F. Allard, D.A. Blom, M.J. Moses, W. Shelton, W. Schneider, Y. Xu, "Catalysis by Design - Theoretical and Experimental Studies of Model Catalysts", SAE-2007-01-1018 (invited).
4. C.K. Narula, M.J. Moses, L.F. Allard, "Analysis of Microstructural Changes in Lean NO_x Trap Material Isolates Parameters Responsible for Activity Deterioration" SAE 2006-01-3420.
5. Y. Xu, W.A. Shelton, and W.F. Schneider, "The thermodynamic equilibrium compositions, structures, and reaction energies of Pt_xO_y (x = 1-3) clusters predicted from first principles," *Journal of Physical Chemistry B*, 110 (2006) 16591.
6. Y. Xu, W. A. Shelton, and W. F. Schneider, "Effect of particle size on the oxidizability of platinum clusters," *Journal of Physical Chemistry A*, 110 (2006) 5839.
7. C.K. Narula, S. Daw, J. Hoard, T. Hammer, "Materials Issues Related to Catalysts for Treatment of Diesel Exhaust," *Int. J. Amer. Ceram. Tech.*, 2 (2005) 452 (invited).

Presentations (last 12 months)

1. Narula, C.K.; Allard, L.F.; Blom, D.A.; Moses-DeBusk, M.; "Bridging the Gap between Theory and Experiments – Nanostructural Changes in Supported Catalysts under Operating Conditions", Society of Automotive Engineers – World Congress, April 2008 (invited).
2. Narula, C.K.; Moses, M.J.; Xu, Y.; Blom, D.A.; Allard, L.F.; Shelton, W.A.; Schneider, W.F.; 'Catalysis by Design – Theoretical and Experimental Studies of Model Catalysts', Nanomaterials for Automotive Applications, Society of Automotive Engineers – international Congress, March 2007 (invited).
3. Blom, D.; Allard, L.; Narula, C.; Moses, M.; "Aberration-Corrected STEM ex-situ Studies of Catalysts" 8/8/07 Wednesday, Microscopy and Microanalysis Meeting, 2007, August 5-9, Ft. Lauderdale, Florida. (Invited).
4. Narula, C.K.; Moses, M.J.; Blom, D.A.; Allard, L.F.; 'Catalysis by Design – Bridging the Gap Between Theory and Experiments– DEER 2007, Detroit, MI
5. Allard, L.F.; Blom, D.A.; Narula, C.K.; Bradley, S.; Catalyst Characterization via Aberration-Corrected STEM Imaging, 20th North American Catalysis Society Meeting, Houston, TX, June 17-22, 2007
6. Blom, D.A.; Moses, M.; Narula, C.K.; Allard, L.F.; Aberration-Corrected STEM Imaging of Ag/Al₂O₃ Lean NO_x Catalyst, 20th North American Catalysis Society Meeting, Houston, TX, June 17-22, 2007

7. Narula, C.K.; Moses, M.; Blom, D.A.; Allard, L.F.; Nano-structural Changes in Supported Pt Catalysts during CO oxidation, 20th North American Catalysis Society Meeting, Houston, TX, June 17-22, 2007
8. Moses, M.; Narula, C.K., Blom, D.A.; Allard, L.F.; Ex-situ Reactor Enabled Microstructural Monitoring: Elucidating Lean NO_x Trap Deterioration Parameters, 20th North American Catalysis Society Meeting, Houston, TX, June 17-22, 2007

Agreement 9105 - Ultra-High Resolution Electron Microscopy for Characterization of Catalyst Microstructures and De-activation Mechanisms

**L. F. Allard, C. K. Narula, P. J. Ferreira, M. J. Yacaman, S. A. Bradley
and C. H. F. Peden**

Objective/Scope

The objective of the research is to characterize the microstructures of catalyst materials of interest for the treatment of NO_x emissions in diesel and lean-burn gasoline engine exhaust systems. The research heavily utilizes new capabilities and techniques for ultra-high resolution transmission electron microscopy with the HTML's aberration-corrected electron microscope (ACEM). The research is focused on understanding the effects of reaction conditions on the changes in morphology of heavy metal species on "real" catalyst support materials (typically oxides), and the understanding of the structures of model mono-, bi- and multi-metallic catalyst systems of known particle composition. With the former systems, these changes are being studied utilizing samples treated in both steady-state bench reactors and a special *ex-situ* catalyst reactor system especially constructed to allow appropriate control of the reaction. Model samples of nanoparticulates of controlled composition on carbon or oxide supports are also being studied in collaboration with the catalysis group at the University of Texas-Austin (Profs. M. Jose-Yacaman and P. Ferreira). Studies of the behavior of Pt species on oxide substrates are also being conducted with colleagues S. A. Bradley of UOP Co., and C. H. F. Peden of PNNL.

Technical Progress

In-Situ electron microscopy: This quarter our in-situ microscopy efforts were directed at both continuing in-situ heating experiments as detailed in the 2nd quarter report, and in developing a new capability for in-situ gas reaction experiments using the concept of an "environmental cell," or "E-cell." This report will focus on the new E-cell concept.

In partnership with Protochips Co. (Raleigh, NC), we have designed a holder for the aberration-corrected JEOL 2200FS "ACEM," which incorporates the MEMS-based heater technology, as previously described, that is essentially a heater chip sandwiched between two ultra-thin (3nm) silicon nitride membranes. These membranes are, like the heater chips, fabricated by semiconductor manufacturing technology over etched windows in silicon chips. The E-cell specimen rod provides gas supply and return tubes from the end of the rod (that is external to the microscope), in to the E-cell heater sandwich, and also the electrical leads to supply power to the heater itself. This assembly is shown in Fig 1. The entire sandwich is retained in the rod tip with o-ring seals, and, in the first prototype we have tested, is only 1.7mm thick. This allows the cell to be inserted within the 2mm gap in the microscope's objective lens pole piece.

In order to test the performance of the E-cell prior to conducting any experiments in our \$3M microscope, we adapted an ion-sputtering deposition (ISD) system in the microscopy lab to accommodate the holder. This was done by affixing the available

airlock assembly from our original ex-situ catalyst reactor system to a machined port in the top plate of the ISD system. Figure 2 shows the E-cell holder inserted into the ISD chamber via the airlock system. The ISD system provides a vacuum in the 10^{-5} Pa range, with rapid pumping via a 280 l/sec turbomolecular pump. With this pumping station, we tested the E-cell holder and showed that it held perfectly against the vacuum, with atmospheric pressure inside the cell.

When doing in-situ reaction experiments, however, we will need to control the gas pressure in many projected experiments to a level in the range of a few Torr (say 10-20 Torr), in order to study the reaction processes in detail at the atomic level. It is a non-trivial exercise to be able to supply gas to such a microvolume, and to know with reasonable precision that the cell contains gas at the required pressure. There are two experimental situations: 1) a controlled static pressure is provided in the cell; and 2) a controlled pressure with some flow is provided in the cell. To accurately control the gas supply to the cell, we designed and constructed a special gas-handling system. Figure 3 is a schematic of the system, and Fig. 4 shows the initial implementation of the system that we have used for preliminary tests. The basic idea is that a scroll pump is used to evacuate a gas supply cylinder into the 10^{-3} Torr range, and also the E-cell holder (the return line will be clamped shut). Initially, the supply cylinder is filled to 1 atm with a purge gas such as nitrogen, and the valves are manipulated to allow several iterations of purging the holder with nitrogen (from atmospheric pressure to vacuum, several times). During a reaction run, say at 10 Torr, the supply chamber is filled to 10 Torr (as measured with a Baratron capacitance manometer on the cylinder), and the valves are manipulated to allow this pressure to equilibrate inside the E-cell. If we need to flow gas thru the cell at a low pressure, an auxiliary cylinder (shown dotted in the schematic) will be appropriately evacuated, and the supply cylinder pressure allowed to flow into the auxiliary cylinder thru a metering valve (not shown). The facility to control the gas pressure to a known level inside the microvolume of the E-cell is critical to the conduct of reaction experiments. It effectively gives us the same capability for gas control as that provided on microscopes dedicated to environmental cell work, in which very expensive differential pumping capabilities and gas manifolds are provided.

Considerations for imaging and gas reactions: As mentioned above, our present cell design sandwiches a heater chip between thin Si nitride windows. While this has been shown to allow pressures up to atmospheric to be used safely, an initial experiment in the microscope showed that the combination of scattering by a 30nm nitride membrane and by air over a 70nm beam path between upper and lower windows causes a severe image degradation such that we will likely not be able to do imaging experiments at a full atmospheric pressure. However, because the Protochips heater allows instantaneous heating and cooling of the sample (the heater membrane is the sample support), if we so desire, we can image a sample under vacuum, then provide the gas to the cell, heat and react for a chosen time, pump the cell back to good vacuum, and iterate the imaging to record changes in the sample that result from the reaction process. We expect that much lower gas pressures, say in the 10 Torr range, will allow imaging unimpeded by scattering within the gas.

A second concern for the best atomic-level imaging with the E-cell is the scattering by a 30nm Si nitride upper window (in STEM mode, the lower window should not affect the image resolution). We have worked out a potential second path to an improved E-cell design, which will allow the heater membrane itself to act as the upper window, with a very thin (10nm) carbon film supported over holes in the heater membrane being the actual seal against the vacuum. We have shown that high-angle annular dark-field (HAADF) imaging thru 10nm of carbon does not materially affect the resolution, so the new design should permit better imaging than our present design. A major impetus to spur this new design is that it will allow a much thinner tip of the E-cell holder, now projected to be 1.4mm. This will be a more comfortable fit inside the microscope's objective lens pole-piece gap, and will preclude the potential that we will damage the pole piece when inserting the holder. The imaging performance of new E-cell will be described in a later report.

References

Status of Milestones

On schedule

Communications/Visits/Travel

L. F. Allard presented an invited seminar at Eastman Chemical Co., Kingsport, TN, entitled "**Looking at Atoms with the Aberration-Corrected Electron Microscope: Applications to Catalyst Characterization.**" This visit has resulted in a Work for Others funded project entitled "**Atomic Scale Imaging of Gas-Metal Cluster Interactions.**"

Publications

"A New MEMS-Based System for Ultra-High-Resolution Imaging at Elevated Temperatures;" L. F. Allard, W. C. Bigelow, M. Jose-Yacaman, D. P. Nackashi, J. Damiano and S. E. Mick, accepted for publication in J. Microsc. Res. & Tech.

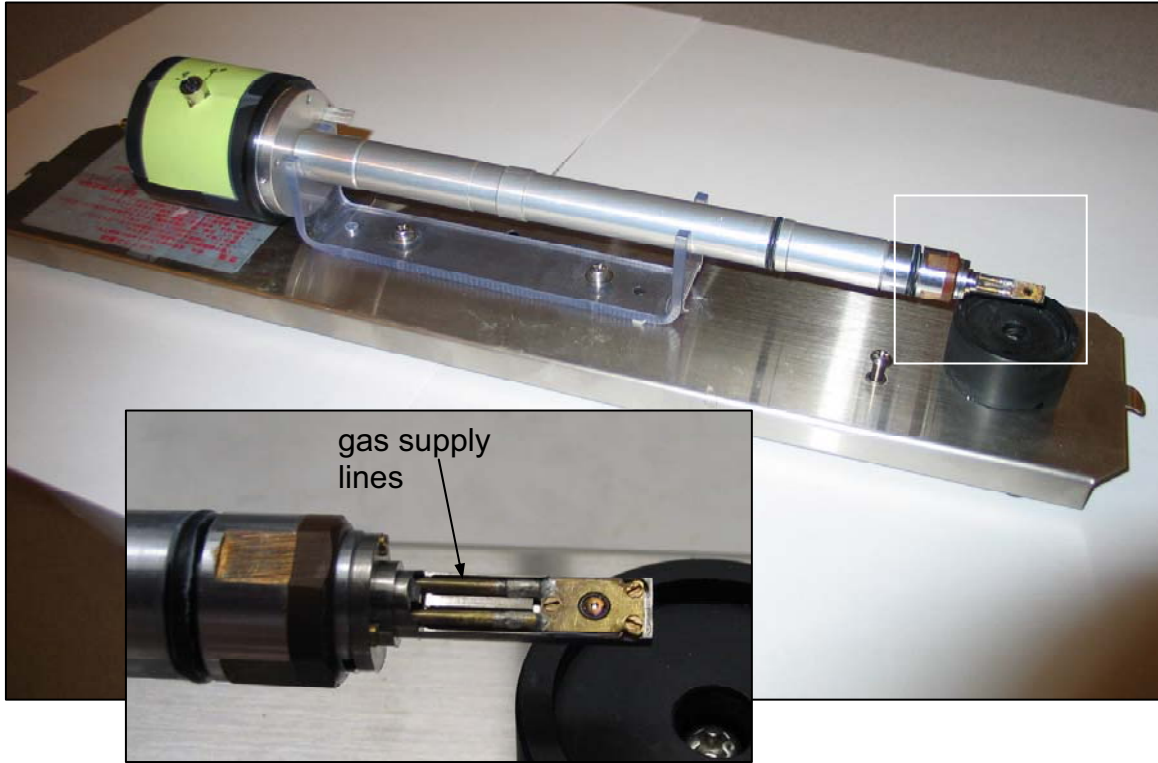


Fig. 1. Prototype E-cell specimen holder for JEOL 2200FS ACEM. The tiny window in the top chip of the stack is clearly visible in the inset photo.

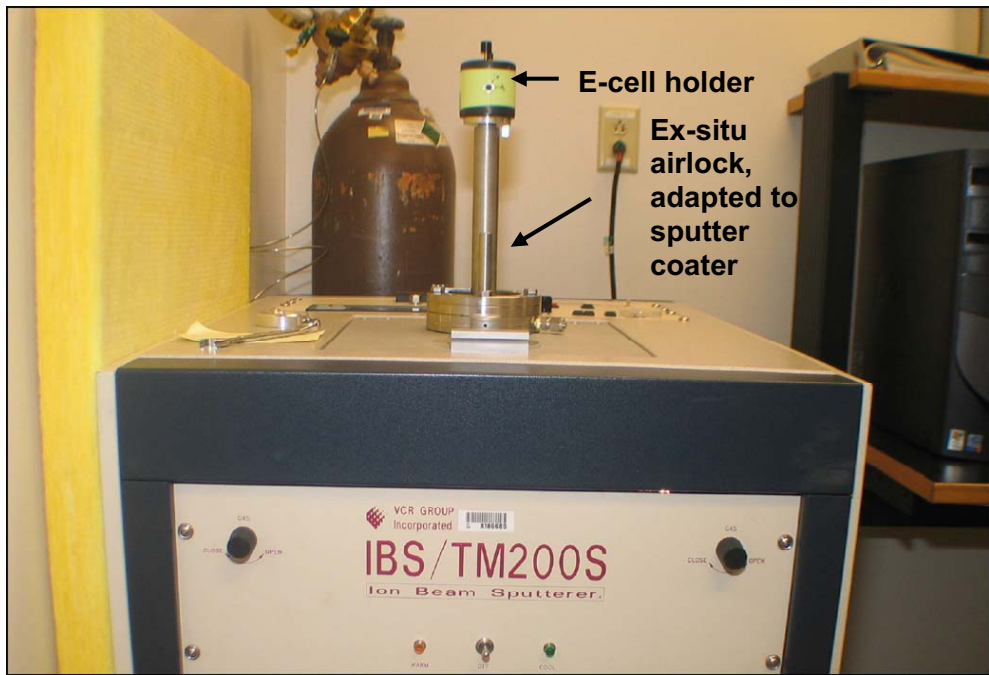


Fig. 2. Ion-beam sputter system with the ex-situ airlock adapted to the top plate of the vacuum chamber. The E-cell holder can be tested under vacuum comparable to the microscope vacuum.

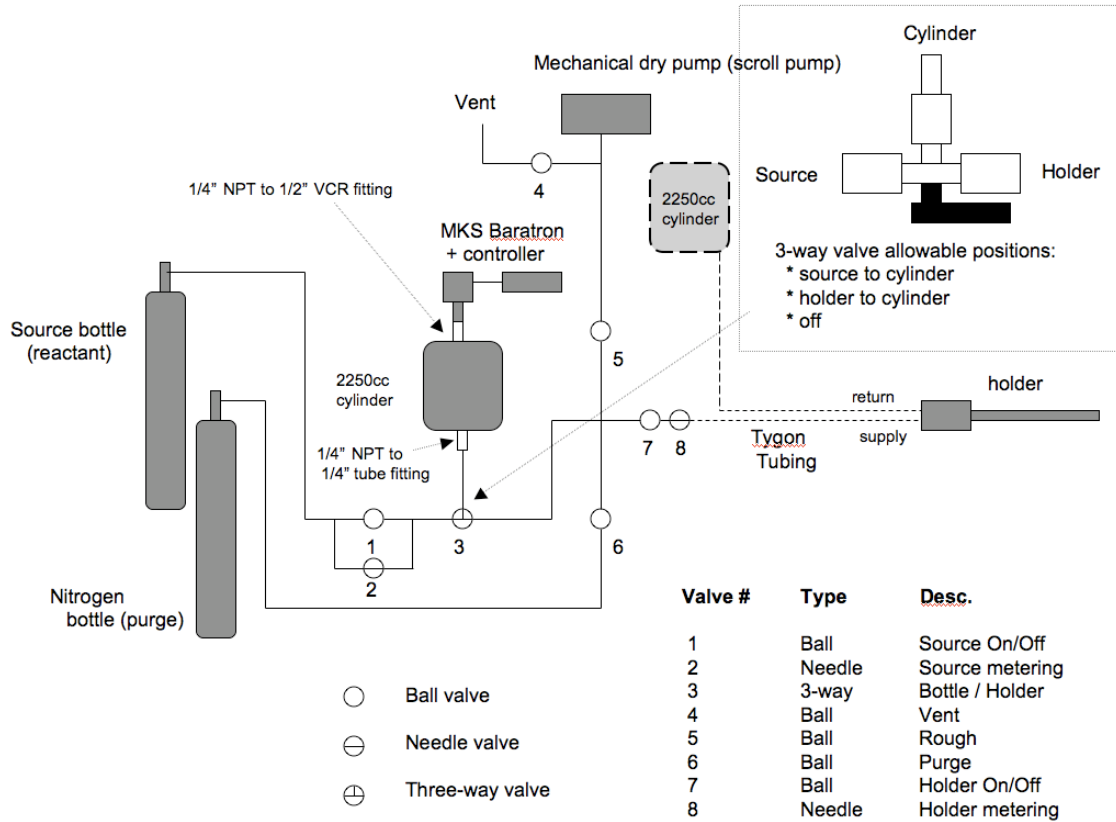


Fig. 3. Sketch of the gas handling system designed to allow either a controlled static pressure in the low Torr regime, or an equivalent pressure with a small flow, inside the environmental cell.

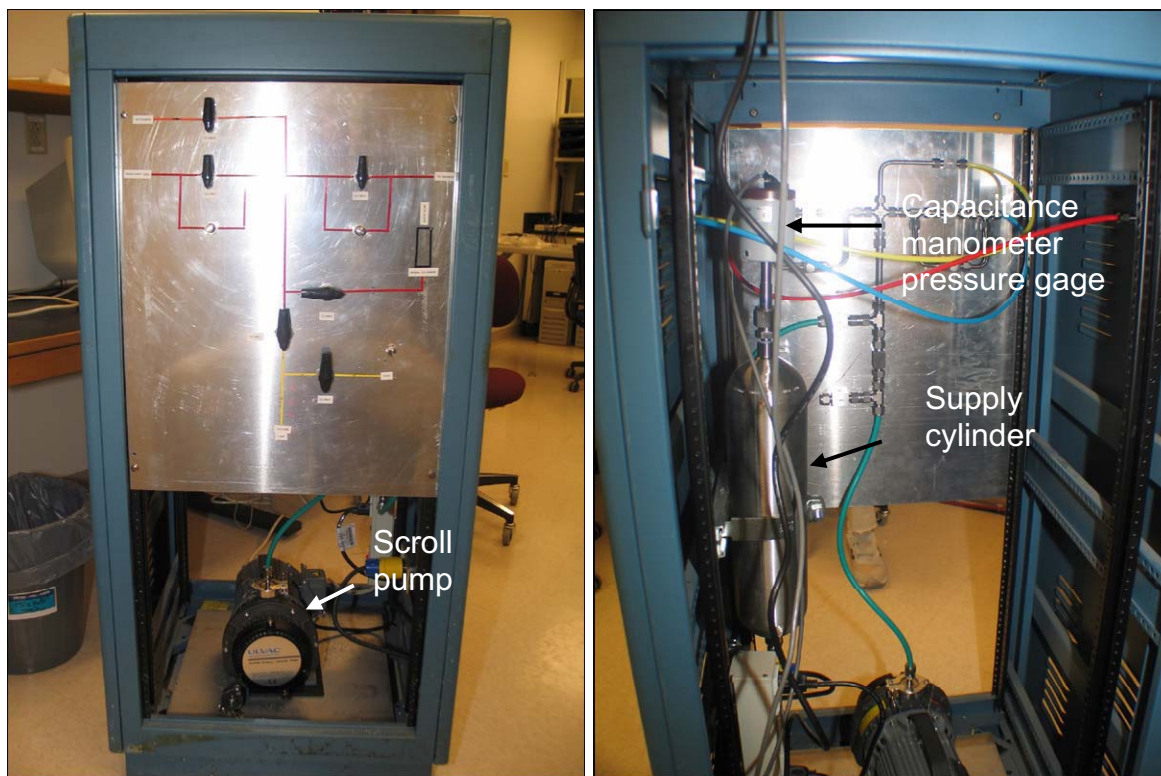


Fig. 4. Front and rear views of the special gas handling system for composition, pressure and flow control in the microvolume of the E-cell holder. Baratron capacitance manometer attached to supply cylinder monitors pressure to cell.

Agreement 9110: Life Prediction for Diesel Engine Components

**H.-T. Lin, T. Kirkland, and A. A. Wereszczak
Oak Ridge National Laboratory**

**N. Philips and J. Jenson
Caterpillar, Inc.**

Objective/Scope

There are four primary goals of this research agreement, which contribute toward successful design and implementation of advanced lightweight material components to achieve high-efficiency engine of 55% of heavy-duty diesel engines by 2012 as set under the 21st CT program: 1) the generation of a mechanical engineering database of candidate advanced lightweight materials before and after exposure to simulated engine environments; 2) the microstructural evolution and accompanied chemical changes during service in these advanced materials; 3) material selection, development, and design of complex-shaped components, and 4) application and verification of probabilistic life prediction methodology for advanced high-efficiency diesel engine components. The methodology implemented would also help to manufacture consistent mechanical reliability and performance of complex shaped components.

Technical Highlights

All valve stems of silicon nitride (both exhaust and intake) valves after 555h natural gas (NG) engine tests were machined into half-cylindrical flexural specimens in order to evaluate the effect of engine environment on the mechanical reliability and corrosion resistance. The mechanical data generated and subsequent SEM analyses for those NG engine tested valve stems provide inputs to end user to verify the life prediction task under the application condition. Mechanical test results showed that there is little or no difference in strength between the intake and exhaust valve stems, in spite of the differences in combustion parameters in each cylinder during the engine operation. Also, these valve stems exhibited characteristic fracture strength of 777 MPa and Weibull modulus of 10.5, which are quite comparable to those measured for the as-received valve stems. In addition, the detailed fractography and SEM analysis showed that the strength limiting flaw of these engine tested valve stems was still mostly due to the presence of those transversely ground surface machining grooves, which were not polished away from the repeatedly reciprocating contact movement between valve stem and guide during the engine test. On the other hand, the engine test was terminated after 555h test. The indirect correlation between life prediction model and experimental results would be the retained mechanical strength. The characteristic strength used for the life prediction is 762 MPa and the predicted failure probability is 5.57×10^{-14} . Thus, the results of the retained fracture strength of these valve stems after 555h engine test indicated that the probability of failure would be equal or less than the predicted probability.

Long-term tensile creep of commercially available TiAl alloys was continued during this reporting period. The test conditions specified are relevant to the temperature and tensile stress profiles imposed on the TiAl turbo wheel under the engine operational

conditions obtained via the FEA modeling task carried out by end users. The database generated from these long-term tensile creep studies will then be used for verification of probabilistic component design and life prediction task critical to end users. The tensile creep data have been updated. The results indicated the creep response of TiAl alloys strongly depends upon the applied stress level and temperature. Also, the microstructure plays a key role in controlling the creep deformation mechanisms as well. These relationships would be identified via the detailed electronic microscopy studies.

Status of FY 2008 Milestones

Complete mechanical and microstructure characterization of TiAl components before and after ACERS diesel engine testing. **(09/08)** – On schedule.

Communications/Visits/Travel

Communications with Dr. J. G. Sun at ANL regarding the correlation between fractography and NDE results for those 555h tested silicon nitride valves.

H. T. Lin attended the 2nd International Congress on Ceramics (ICC-2), June 29-July 4, 2008, Verona, Italy.

Problems Encountered

None.

Publications/Presentations/Awards

H. T. Lin, "Advanced Silicon Nitride Ceramics for Heavy-Duty Diesel Engine Applications," invited paper, presented at the 2nd International Congress on Ceramics (ICC-2), June 29-July 4, 2008, Verona, Italy.

References

None

Agreement 14957: Thermoelectrics Modeling

**A. A. Wereszczak, T. P. Kirkland, H. Wang, and W. L. Daloz
Oak Ridge National Laboratory**

Objective/Scope

Measure needed thermomechanical and thermophysical properties of candidate thermoelectric (TE) materials and then use their data with established probabilistic reliability and design models to optimally design automotive and heavy vehicle TE modules. Thermoelectric materials under candidacy for use in TE modules tend to be brittle, weak, and have a high coefficient of thermal expansion (CTE); therefore, they can be quite susceptible to mechanical failure when subjected to operational thermal gradients. A successfully designed TE module will be the result of the combination of temperature-dependent thermoelastic property and strength distribution data and the use of the method of probabilistic design developed for structural ceramics.

Technical Highlights

Characterization of the p- and n-type bismuth telluride continued during the present reporting period. Materials were purchased and cut to into shape by Marlow Industries, Inc., Dallas, TX. This thermoelectric material is mature and its testing will provide a reference database that can be used to compare developmental thermoelectric materials too. The measurements of Young's Modulus, Poisson's ratio, CTE, thermal conductivity, and uniaxial and biaxial flexure strength as a function of temperature have all commenced. The large number of specimens enables the generation of statistically significant strength data. Any anisotropic variation of E, ν , CTE, and strength is under exploration. Fractography of tested strength specimens is underway and failure initiation sites and strength-limiting flaw types are being identified. The uniaxial and biaxial flexure strength test methods will enable us to censor the data according to edge-type and surface-type, and perhaps even volume-type flaws.

This quarterly report chronicles, flexure strength, dilatometry, and thermal conductivity testings.

The three-point flexure test setup is shown in Fig. 1 and the summary of that room temperature test matrix is listed in Table I. The "R-Z" orientation for both the p- and n-type materials were approximately twice as strong as the "R-R" orientations. For a given orientation, there was not a discernable strength difference between the p- and n-type materials. Lastly, the 2 mm dimensions were prepared using two different slicing processes, and they were found to produce similar strengths. Fractography is now underway to identify strength-limiting flaw locations and types and to enable strength censoring. 225°C strength testing is presently underway.

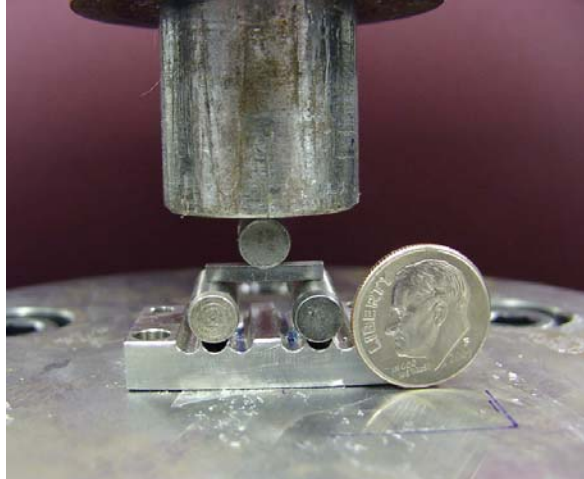


Figure 1. Three-point flexure strength test fixture and bismuth telluride specimen.

Table I. Summary of Three-Point Flexure Inert Strengths. 12.7 mm span used. Nominal specimen dimensions were 2 x 2 x 15 mm.

Type	Orientation	Tension Surface	Number of Specimens	Average Max Stress (MPa)	Std Dev (MPa)
P	R - R	As Mach	15	38.2	8.5
P	R - R	Cut	12	38.6	3.1
P	R - Z	As Mach	16	80.9	5.4
P	R - Z	Cut	17	79.4	4.1
N	R - R	As Mach	16	45.7	5.2
N	R - R	Cut	17	45.0	3.8
N	R - Z	As Mach	17	79.5	8.0
N	R - Z	Cut	17	81.1	8.1

The equibiaxial (ring-on-ring) flexure test setup is shown in Fig. 2 and the summary of that room temperature text matrix is listed in Table II. Only p-type material was available for this specimen geometry. Again, the “R-Z” orientation for both the p- and n-type materials was significantly stronger than the “R-R” orientation - about 50% stronger. Polished test specimens were also prepared for both orientations and tested in flexure; however, their produced strengths were minimally stronger than their as-ground counterparts. Fractography is now underway to identify strength-limiting flaw locations and types and to enable strength censoring.



Figure 2. Ring-on-ring equibiaxial flexure strength test fixture and bismuth telluride specimen.

Table II. Summary of Equibiaxial Flexure Inert Strengths. 6.35 and 12.7 mm ring diameters used. Nominal specimen dimensions were 15 x 15 x 2 mm.

Type	Orientation	Surface Condition	Number of Specimens	Average Failure Stress (MPa)	Std Dev (MPa)
P	R - R	As-Ground	25	29.9	2.2
P	R - Z	As-Ground	25	43.5	3.1
P	R - R	Polished	11	31.9	2.1
P	R - Z	Polished	15	47.6	4.6

Dilatometry of p- and n-type bismuth telluride was completed. Testing ranged between room temperature and 240°C. Because the thermoelectric properties of this material are known to exhibit transverse anisotropy, test coupons were sectioned in both orientations from both the p- and n-type materials, and this enabled our study of thermal expansion as a function of orientation. Three specimens were tested per condition to examine repeatability. As shown in Table III, the average CTE for the “R-R orientation” was approximately 30% higher than the “R-Z orientation” for the p-type material and about 20% higher for the n-type. Results were for a given test condition were quite repeatable.

Table III. Summary of Equibiaxial Flexure Inert Strengths. 6.35 and 12.7 mm ring diameters used. Nominal specimen dimensions were 15 x 15 x 2 mm.

Type	Orientation	Specimen Number	Average CTE up to 240°C (ppm/°C)
P	R - R	1	18.9
P	R - R	2	18.7
P	R - R	3	18.8
P	R - Z	1	14.3
P	R - Z	2	13.9
P	R - Z	3	13.8
N	R - R	1	17.1
N	R - R	2	17.3
N	R - R	3	17.3
N	R - Z	1	14.7
N	R - Z	2	14.4
N	R - Z	3	14.3

Thermal conductivity of the Marlow materials was tested using laser flash diffusivity and differential scanning calorimeter (DSC). Table VI shows a summary of room temperature properties. Figure 3 shows specific heat of both n-type and p-type materials from 10K to 500K. The low temperature data were obtained using a Quantum Design PPMS and the high temperature data from DSC. The discontinuity between low temperature and high temperature curves near room temperature was caused by instrument response. We used Debye-based model to fit the curve in calculating thermal conductivity. Thermal conductivity of both n-type and p-type materials are shown in Figure 4.

Table IV. Average room temperature thermal properties and dimensions of 5 N-type and 5 P-type bulk thermoelectrics.

	N-type	P-type
Thermal Diffusivity (cm ² /sec)	0.011	0.011
Thickness (mm)	1.024	1.023
Diameter (mm)	9.530	9.488
Weight (g)	0.561	0.479
Density (g/cm ³)	7.683	6.630
Cp (J/gK)	0.159	0.186
Thermal Conductivity (W/mK)	1.344	1.356

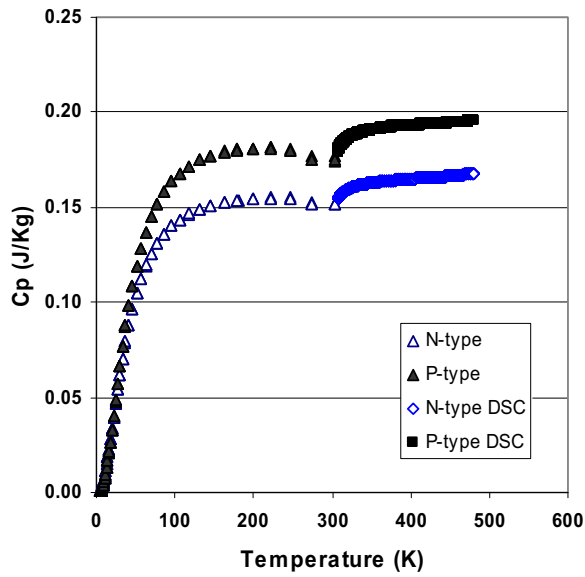


Figure 3. Specific heat of n-type and p-type materials from 10-500K.

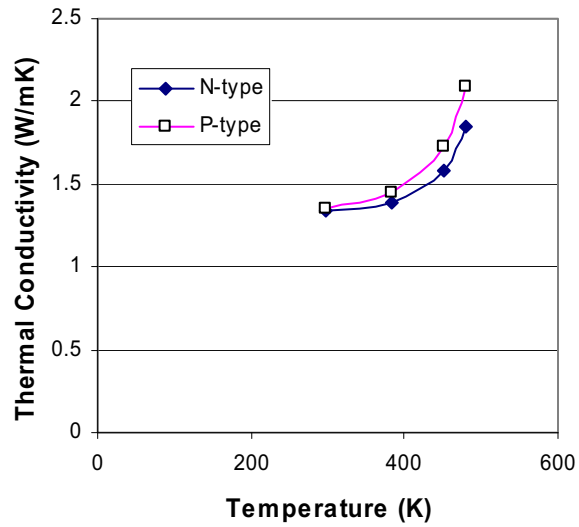


Figure 4. Thermal conductivity of n-type and p-type bismuth telluride

Status of FY 2008 Milestones

Generate thermomechanical property database on a candidate p- and n-type thermoelectric materials that will be used to model and predict probabilistic reliability of a TE device. [09/08] *On schedule.*

Communications/Visits/Travel

Wereszczak and Wang visited Marlow Industries, Dallas, TX on 24 April 2008.

Numerous communications occurred between Wereszczak and Marlow's J. Sharp during the present reporting period.

Problems Encountered

None.

Publications/Presentations/Awards

None.

References

None.

Agreement 16308: Thermoelectric Materials

David J. Singh
Oak Ridge National Laboratory

Objective/Scope

We will use modern science based materials design strategies to find ways to optimize existing thermoelectric materials and to discover new families of high performance thermoelectrics for waste heat recovery applications. The emphasis will be on the thermoelectric figure of merit at temperatures relevant to waste heat recovery and on other properties important for applications, especially anisotropy and mechanical properties.

Technical Highlights

Oxide and Chalcogenide Materials:

The focus of this work is to identify oxide and chalcogenide materials that offer a combination of high thermoelectric performance and applicability to vehicular applications. A key consideration that is special for vehicles is that the materials must be at least potentially inexpensive. We completed our calculations for $YCuO_2$ in the delafossite structure using first principles methods. [1,2] This oxide material meets the requirements of having low cost ingredients and at the same time offering high thermopower. Results were communicated to C. Narula (ORNL) and to General Motors. A technical report on this subject, discussing in particular the potential application of this material to waste heat recovery, was published in Physical Review.

As discussed in the FY2008 Q1 and Q2 reports, we have been performing first principles electronic structure and Boltzmann transport calculations to evaluate the potential for using La-Te phases for waste heat recovery. We found good correspondence between our calculated results and the experimental data taken by J. Snyder and collaborators at the California Institute of Technology. In particular we were able to explain why the doping dependence of the thermopower when going to low carrier concentrations was weaker than normal. This results from two band behavior in the electronic structure. A technical report on this subject is being prepared.

Jihui Yang from General Motors contacted us and indicated interest in the vibrational properties of PbTe. This is a material that GM is interested in as a thermoelectric for waste heat recovery. Based on this, we performed detailed first principles calculations of its vibrational properties. Understanding the very low thermal conductivity of materials related to PbTe is a long standing challenge. In particular this material has only two atoms per unit cell, no obvious rattling ion, and a highly symmetric structure. Nonetheless, when nanostructured, it can display exceedingly low thermal conductivity. We found that there is a zone center polar soft mode (see Fig. 1), indicative of nearness to ferroelectricity. Significantly, we find that the soft mode is very anharmonic and is strongly coupled to strain and to the heat carrying longitudinal acoustic vibrational modes. This partly explains why nanostructured PbTe based materials, such as the "LAST" phases are such effective thermoelectrics. Besides providing a framework for understanding the properties of PbTe, this result shows that the vibrational properties

are strongly dependent on strain. This suggests that besides nanostructuring, materials modifications that induce local strains can also be used to control the properties of PbTe based materials. These results were communicated to Jihui Yang at General Motors and a technical report is being finalized.

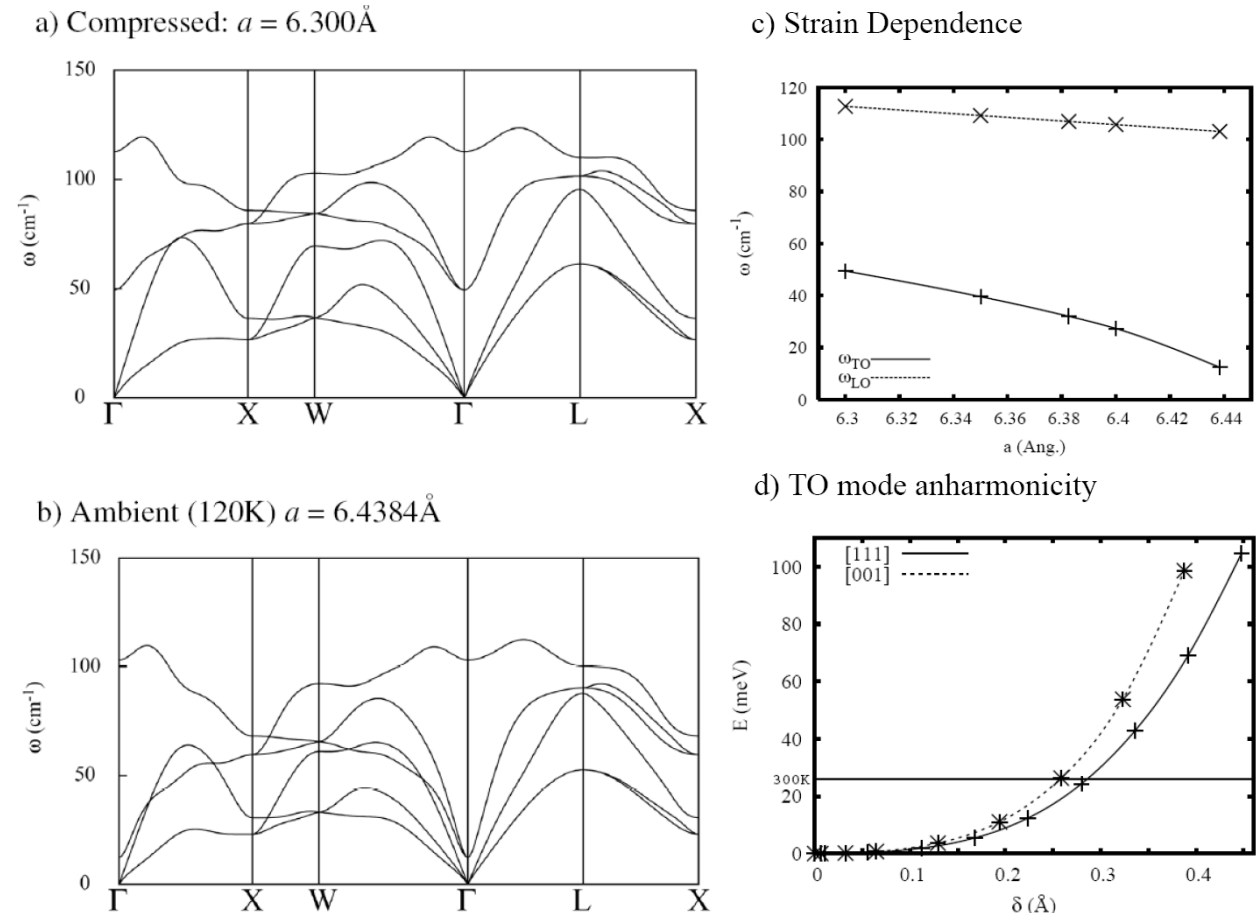


Fig 1: Calculated phonon dispersions of PbTe (this is the momentum dependent vibrational spectrum of a solid) at two lattice parameters (a,b), dependence of the zone center optic mode frequencies on compressive strain (c) and transverse optic mode anharmonicity (d). The results show strong anharmonic coupling between the soft optic mode and the heat carrying longitudinal acoustic modes.

Status of FY 2008 Milestones

We are progressing towards our milestone of predicting a new thermoelectric composition. Strategies that will be used are to continue investigation of spinel based titanates, Cu containing delafossites, and rare-earth chalcogenides. Depending on the results we will continue with those materials and/or investigate alternate narrow band oxides containing mixed-valent transition element ions.

Communications/Visits/Travel

1. D.J. Singh: Presented invited talk at European MRS Meeting, Strasbourg, France on Thermoelectric Materials.
2. D.J. Singh: Travel to Pasadena, California to present colloquium on thermoelectric materials at California Institute of Technology and to collaborate with J. Snyder (Caltech) on La-Te thermoelectrics.

Problems Encountered

No significant problems encountered this quarter.

Publications/Presentations/Awards

Publications:

1. D. J. Singh, "Band structure and thermopower of doped YCuO_2 ", *Physical Review B* **77**, 205126 (2008).

References

1. D. J. Singh and L. Nordstrom, *Planewaves, Pseudopotentials and the LAPW Method*, 2nd Edition, Springer, Berlin, 2006.
2. G.K.H. Madsen and D. J. Singh, "BoltzTraP: A code for calculating band-structure dependent quantities", *Computer Physics Commun.* **175**, 67 (2006).